ELSEVIER

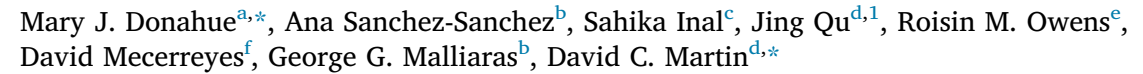
Contents lists available at ScienceDirect

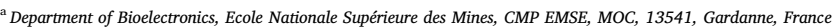
Materials Science & Engineering R

journal homepage: www.elsevier.com/locate/mser



Tailoring PEDOT properties for applications in bioelectronics





- b University of Cambridge, Dept. of Eng., Electrical Eng. Division, 9 JJ Thomson Avenue, Cambridge, CB3 0FA, UK
- ^c Division of Biological and Environmental Sciences and Engineering, King Abdullah University of Science and Technology (KAUST), Thuwal, 23955, Saudi Arabia
- d Department of Materials Science and Engineering, University of Delaware, 19716, USA
- ^e Department of Chemical Engineering and Biotechnology Philippa Fawcett Drive, CB30AS, Cambridge, UK
- f POLYMAT, University of the Basque Country UPV/EHU, Joxe Mari Korta Center, Avda. Tolosa 72, 20018, Donostia-San Sebastian, Spain

ARTICLE INFO

Keywords: Bioelectronics PEDOT Conducting polymer Material properties Biointerfacing applications

ABSTRACT

Resulting from its wide range of beneficial properties, the conjugated conducting polymer poly(3,4-ethylene-dioxythiophene) (PEDOT) is a promising material in a number of emerging applications. These material properties, particularly promising in the field of bioelectronics, include its well-known high-degree of mechanical flexibility, stability, and high conductivity. However, perhaps the most advantageous property is its ease of fabrication: namely, low-cost and straight-forward deposition processes. PEDOT processing is generally carried out at low temperatures with simple deposition techniques, allowing for significant customization of the material properties through, as highlighted in this review, both process parameter variation and the addition of numerous additives. Here we aim to review the role of PEDOT in addressing an assortment of mechanical and electronic requirements as a function of the conditions used to cast or polymerize the films, and the addition of additives such as surfactants and secondary dopants. Contemporary bioelectronic research examples investigating and utilizing the effects of these modifications will be highlighted.

1. Introduction

In recent years, conducting polymers have gained attention as their flexible and conformable material characteristics are valuable for the emerging field of organic electronics. Among conducting polymers, poly(3,4-ethylenedioxythiophene) (PEDOT) has been at the forefront of rapid development in this area, contributing significantly to an extensive new realm of applications for flexible and stretchable electronics [1,2]. This expanding field includes a long list of applications, including stretchable integrated circuits [3], active matrix displays [4,5], stretchable solar cells [6,7], and light emitting diodes [8]; all relying on good electronic conductivity and the tunable mechanical properties of the active material [9,10]. A more specific domain in which flexible and conformable material characteristics are particularly beneficial is the field of bioelectronics. Soft, compliant material properties can better match biological systems, significantly improving the interface between biological tissue and electronic devices while

avoiding detrimental effects [11–13]. Specific applications include wearable sensors, robotics, hemispherical eye cameras, implants, and artificial tissue [14]. To achieve the material properties required for applications such as these, low tensile moduli are needed to achieve good performance over the large range of deformations regularly exhibited by biological systems [15]. Although a few promising conductive and flexible organic materials exist, the field of bioelectronics has well-demonstrated the potential of poly(3,4-ethylenedioxythiophene) (PEDOT) through a great deal of application-specific success [14,16,17].

Here we aim to review the role of PEDOT in addressing the assortment of mechanical and electronic requirements for flexible/stretchable electronics, particularly in the case of bioelectronics where mixed ionic/electronic conduction is valuable [14,18–20]. The properties of PEDOT films depend strongly on the chemical structure of the polymer, the conditions used to cast or polymerize the films, and the presence of additives such as surfactants and secondary dopants [7]. In

^{*} Corresponding authors.

E-mail addresses: mary.donahue@emse.fr (M.J. Donahue), ana_sanchez@ehu.eus (A. Sanchez-Sanchez), sahika.inal@kaust.edu.sa (S. Inal), jingq@udel.edu (J. Qu), rmo37@cam.ac.uk (R.M. Owens), david.mecerreyes@ehu.es (D. Mecerreyes), gm603@cam.ac.uk (G.G. Malliaras), prilty@udel.edu (D.C. Martin)

¹ Present address: Advanced Materials Characterization Lab, 151 Interdisciplinary Science and Engineering Laboratory, University of Delaware, Newark, DE 19716.

previous work, PEDOT films prepared from common formulations and methods tended to degrade under strain (i.e. crack formation), failed to maintain good electrical properties when exposed to pressure or temperature changes, or delaminated over time [19,21,22]. Strategies have therefore been developed to ensure that mechanical durability coexists with electrical conductivity. It is the intention of following sections to cover these variations and the resulting mechanical and electrical properties. Section 2 will focus on the polymerization methods and Section 3 will cover specific methods to improve mechanical and electrical properties of the resulting PEDOT films. Important contemporary research examples investigating and utilizing the effects of these modifications for bioelectronic applications will be highlighted in Section 4.

2. Polymerization methods for PEDOT

PEDOT is currently one of the most successful conducting polymers (CPs) from both a fundamental and practical perspective. This success is a result of its thermal, electrochemical, and moisture stability, as well as the high conductivity, optical transparency, and low oxidation potential. The mechanical and electrical properties of PEDOT may be finetuned through the use of various counterions, secondary dopants or additives, polymeric blending, variation of processing parameters, and the use of post-treatment methods. By taking advantage of this variability, PEDOT-based films may be tailored to suit a variety of applications. In this section, the methods to polymerize PEDOT will be discussed, along with the associated advantages/disadvantages of these methods. Example film variations resulting from the these techniques will be presented.

2.1. Polymerization methods

PEDOT is oxidized in its conductive state possessing positive charge carriers. In order to compensate for these positive charges, or *holes*, negatively charged counterions are utilized during the polymerization

process. These counterions include low molecular weight anions, such as hexafluorophosphate (PF₆⁻) [23,24], perchlorate (ClO₄⁻) [25], or tosylate (Tos) [26-30], polymeric counterions such as polystyrene sulfonate (PSS) or sulfated poly(B-hydroxyethers) (S-PHE) [31,32], or biopolymers such as hyaluronic acid, dextran, or heparin [33]. Often, these counterions are called dopants; however, this term can be a misleading analogy to inorganic electronics as they do not dope PEDOT in the traditional sense [34,35]. Salts of the counterion, or salts of the oxidizing agent in presence of the counterion, are utilized during the polymerization process. The anions incorporated into the resulting doped PEDOT film thus balance the positive charge carriers. The PEDOT polymerization and oxidation reaction is typically carried out through one of three methods: electrochemical polymerization, wet chemical oxidative polymerization, or vapor phase polymerization (VPP) (Fig. 1). These techniques have a variety of advantages and disadvantages regarding deposition as well as the resulting film properties. An overview of these qualities will be given here.

2.1.1. Electrochemical polymerization

Electrochemical polymerization of PEDOT is carried out through the electrochemical oxidation of the EDOT monomer in the presence of the counterion. As the counterions are typically present in the reaction solution in the form of salts, this polymerization process facilitates a wide range of possibilities. The choice of counterion influences the resulting surface morphology, the electrical and mechanical properties of the polymer film, and the oxidation level of PEDOT [36,37]. Furthermore, the parameters of electrochemical polymerization, such as deposition method (i.e. cyclic voltammetry (CV), potentiostatic, galvanostatic, or pulsed deposition), scan speed, deposition charge density, or utilized solvent significantly affect the final polymer [38]. A visual demonstration of these effects is given in Fig. 2, including an example in which the influence of small anions such as ClO_4^- , PF_6^- (Fig. 1a), in addition to variation of the cation (Li+, TBA+), during electropolymerization was investigated by Melato et al. [39]. It was shown that LiClO₄ leads to a higher electropolymerization efficiency as well as

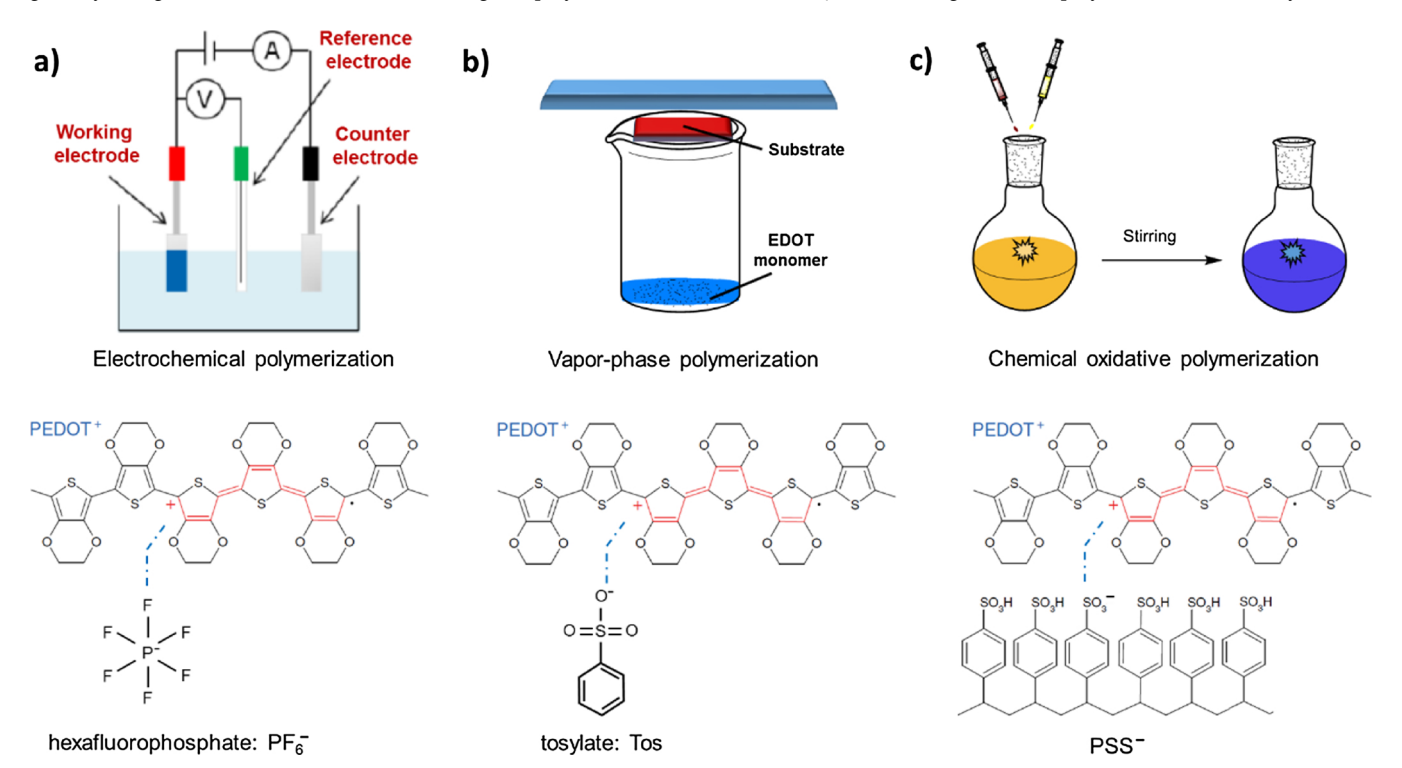


Fig. 1. Various polymerization reactions for PEDOT. **a)** Electrochemical polymerization with a low molecular weight counterion example, hexafluorophosphate (PF₆⁻). **b)** Vapor phase polymerization with the commonly used tosylate (Tos) counterion. **c)** Chemical oxidative polymerization with the chemical structure of polyanion polystyrene sulfonate (PSS).

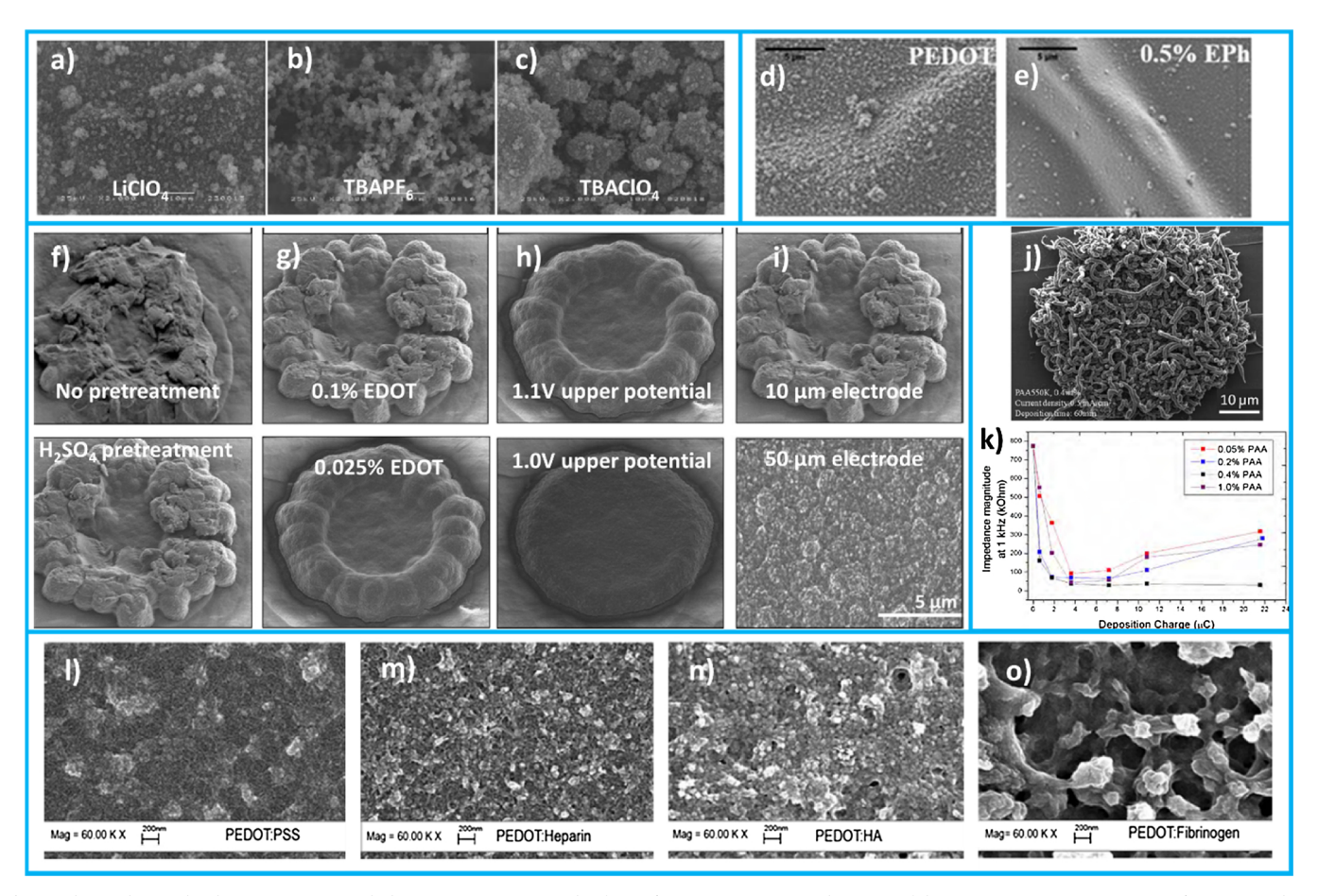


Fig. 2. Electrochemical polymerization. Morphology variation as a result of (a), (b), (c) counterion and cation (of the counterion) variation [39], (d) no use and (e) use of co-polymer EPh [40], (f) acid treatment of electrode surface, (g) EDOT monomer concentration, (h) applied polymerization potential, (i) electrode size (i.e. charge density) [38], and (j) PAA present during polymerization using LiClO₄ with (k) observed electrochemical impedance values [44]. Various biopolymer counterion use and resulting morphologies: (l) PSS (for comparison), (m) heparin, (n) hyaluronic acid, and (o) fibrinogen [48]. Blue borders group images from specific studies. Reproduced with permission of: [39,40,38,44,48] (For interpretation of the references to colour in this figure legend, the reader is referred to the web version of this article.).

an increased crystallinity and electroactivity of the polymer. The ClO₄counterion results in clusters of different sizes and promotes the formation of a more compact morphology (Fig. 2a,c), whereby the film porosity increases when the larger cation TBA + is used in place of Li +. The porosity of the PEDOT film obtained with TBA+ and the PF6counterion is further increased, resulting in a fibrous structure (Fig. 2b). A similar morphology using TBAClO₄ was demonstrated by Ouyang et al. in a study on the modification of mechanical properties upon introduction of a co-polymer [40]. The co-polymerization with 1,3,5-tri [2-(3,4-ethylenedioxythienyl)]-benzene (EPh) in this example (Fig. 2d, e) leads to a more compact crosslinked structure with improved mechanical strength, demonstrated through AFM nanoindentation tests (see Tables 1 and 2 on mechanical characterization techniques). The examples so far involve the use of small counteranions, however electrochemical polymerization of EDOT may also be carried out in the presence of polymeric counterions, as is the case in Fig. 2f-j using PSS. Yamato et al. were the first to report on the electrochemical polymerization of EDOT from an aqueous PSS solution [41]. This polymer was later shown to have high electrochemical stability, particularly when compared with polypyrrole (PPy). Interestingly, an alternative polymeric counterion dopant S-PHE was shown to improve the mechanical stability of free-standing films, with film lengths up to 20 m reported [31,42].

Differences in PEDOT:PSS film morphology due to variation of the electropolymerization potential, upper scan limit for potential scan deposition, EDOT monomer concentration, $\rm H_2SO_4$ pre-treatment of

substrates, and current density are clearly seen in Fig. 2f-i (it should be noted that best conditions of each process variation were chosen, resulting in duplicate images, for example 2f bottom and 2g top). These effects were investigated by Castagnola et al. [38] to optimize mechanical and electrical properties of neural recording electrodes, a bioelectronics application that has shown great potential for PEDOTbased films. An evaluation parameter often employed to indicate how effectively electrodes record or stimulate excitable cells is the electrochemical impedance [43]. Low impedance values are desired, which result from high surface area, in addition to high mobility of ions within the bulk of the polymer film. These advantageous attributes make the increased surface area of the structured film in Fig. 2j theoretically interesting for implantable neural applications. Here, EDOT was polymerized electrochemically using LiClO₄, analogous to the film in Fig. 2a, however in this case in the presence of polyacrylic acid (PAA) [44]. Although it was shown that PAA does not act as the counterion in this instance, with only ClO₄ remaining in the final film to play this role, it may be seen in Fig. 2k that the amount of this acid present during polymerization affects the resulting impedance of the final film. Despite the beneficial increase of electrode surface area due to the fibrillary film structure, it is possible that the polymer protruding from the surface may cause delamination issues for implantable applications [45]. Indeed, delamination of electropolymerized films has been observed as a result of such mechanical friction for thick films, in addition to substrate dependent adhesion problems [22,46,47]. Methods to improve these issues are discussed in Section 3.1.1.

Table 1
Characterization methods for cohesion of CP films.

	Film type	Measured Properties	Summary of the method	
Tensile test (free-standing film) [18,142]	Chemically polymerized	Stiffness, strength, fracture strain	The most direct mechanical testing method; requires a free standing thick film (several microns), which is difficult to acquire.	
Tensile test (on water surface) [143,15]	Chemically polymerized	Stiffness, strength, fracture strain, yield point	Capable of measuring ultrathinspin cast films. Experimental setup is complicated and difficult. The effect of water on the mechanical properties of the films has not been carefully studied yet.	
Nanoindentation [144]	Chemically and electrochemically polymerized	Stiffness	Capable of measuring the film with the substrate attached. Obtained values are dependent on the tip geometry and surface roughness.	
AFM indentation [40,145]	Chemically and electrochemically polymerized	Stiffness	Capable of measuring the film with the substrate attached; not able to provide the strength information. The value is dependent on the spring constant of the cantilever and the calibration method.	
Thin film cracking (tensile test) [145]	Chemically and electrochemically polymerized	Stiffness, strength, fracture strain	Requires deposition of the film on a ductile substrate. The effect of the interface has not been carefully studied yet.	
Buckling method [7,146]	Chemically polymerized	Stiffness, yield point	Requires depositing the film on a ductile substrate. Not able to provide the tensile strength. $\ \ \ \ \ \ \ \ \ \ \ \ \ \ \ \ \ \ \$	

 Table 2

 Characterization methods for substrate adhesion of CP films.

	Film type	Measured Properties	Summary of the method
Pull-off test [147,148]	Chemically and electrochemically polymerized	Adhesion fracture energy	Requires a second, stronger adhesive interface that does not permeate the film, affecting the first. Challenging for thin films.
Composite bending test [149]	Chemically and electrochemically polymerized	Cohesion energy	An indirect method that measures the adhesion of the bonded interface between elastic sheets. In some cases bending is not sufficient to crack the film.
Thin film cracking (loop test) [150]	Chemically and electrochemically polymerized	Relative shear strength	An indirect method to measure the ratio of interfacial shear strength and shear strength, with a critical value of 1 providing an indicator of the potential failure mode.

2.1.1.1. PEDOT:Biopolymer. Biopolymers are a subset of counterions that are particularly interesting for bioelectronics. As early as 1998, electrochemical polymerization of peptides was applied to glassy carbon electrodes by Huber et al., demonstrating in vivo nerve cell attachment to implanted electrodes. In aspiration of achieving similar beneficial effects regarding tissue interfacing, early studies on CPs were carried out to incorporate biomolecules in PPy matrices through electrochemical polymerization [48]. Building on the studies using PPy (as often the case), this technique was later applied to create PEDOT:biomolecule electrode materials through the incorporation of an anionic biopolymer, playing the role of the counterion. As a result of the discussed ease of counterion exchange in electrochemical polymerization, many PEDOT:biopolymer examples to date have been generated through this polymerization process.

Amoung the numerous negatively charged biopolymers that have been employed as counterions for the electrochemical polymerization of PEDOT are adenosine 5'-triphosphate (ATP), fibrinogen, guar gum, carboxymethyl cellulose, DNA, xanthan gum, pectin, Glycosaminoglycans (GAGs) such as heparin, hyaluronic acid, and chondroitin sulfate; all demonstrating potential due to their non-toxicity. The initial PEDOT:biopolymer reported by Cui et al. in 2003 utilized bioactive peptide complexes on neural probes [49]. The counterion peptide sequence DCDPGYIGS resulted in high-quality neural recordings using the modified electrode sites. In 2008, an in vitro study of PEDOT:ATP electrodes was carried out by Xiao et al. to demonstrate improved neural (PC12) cell adhesion in comparison to PEDOT:LiClO₄. The authors proposed the use of PEDOT:ATP as a potential neural implant material [50]. Also particularly focused on improving implantable neural interfaces, Asplund et al. have investigated a variety of PED-OT:biopolymer complexes to improve the implant/tissue interaction [33,51,52]. The various morphologies resulting from different biopolymers are compared to that using PSS in Fig. 21-o. In 2011, Lv et al. provided results on the electroactivity of PEDOT films doped with anionic polysaccharides. Although no specific biological application was targeted, good electrochemical properties were demonstrated in comparison to (some) standard counterions as well as good texture and adhesion properties on ITO [53].

In general, it is evident that variation of counterion and electrochemical polymerization parameters affect the polymer film properties. Taking this effect into consideration, it may naturally be assumed that using alternative polymerization processes (vapor phase or chemical oxidative polymerization) will further affect the film. These alternative polymerization processes and example polymer films will be discussed in the following two sections.

2.1.2. Chemical oxidative polymerization

Whereas electrochemical polymerization induces oxidation of the EDOT monomer through the application of an electric potential, chemical oxidative polymerization utilizes chemical oxidation to induce this polymerization process. A wide variety of PEDOT:counterion composites is also possible by chemical polymerization; however, the counterions practically employed are fewer in number compared to electrochemical polymerization. This limitation is a result of the utilized salt typically performing the dual role of oxidizing agent to induce polymerization as well as providing the counterion for the PEDOT complex. In the initial work on chemical oxidation of PEDOT from Jonas and Schrader, many possibilities for oxidation agent possibilities were given based on their low-cost and ease of handling [54]. These options include FeCl₃, Fe(ClO₄) and the iron(III) salts of organic acids and of inorganic acids containing organic radicals, H₂O₂, K₂Cr₂O₇, alkali metal or ammonium persulphates, alkali metal perborates, and potassium permanganate [54]. The chosen oxidant influences, among other things, the polymerization kinetics, which in turn have an effect on the PEDOT deposition and the resulting film properties. For example, extremely fast polymerization rates may give rise to unwanted side reactions and result in partial conjugation of polymer chains or precipitates within the solution [55]. Rate-controlling additives, such as imidazole, pyridine, or triblock copolymers (i.e. poly(ethylene glycol)block-poly(propylene glycol)-block-poly(ethylene glycol) or PEG-PPG-PEG), may be employed in this case to slow the process and give films with desirable properties [30,55-58]. Conversely, extremely low rates may need an additional catalyst to polymerize the film, but are practical due to straightforward addition of co-polymers, co-solvents, or other additives to a single solution (Fig. 5, Section 3) [54].

Overall, a large parameter space is available to tune and optimize chemically polymerized PEDOT films for the intended application. The available parameters include the monomer and its concentration, a variety of oxidants (i.e. counterions), additives and their concentrations, and additional factors such as humidity, temperature, and the utilized solvent. To date, the most often used and studied oxidizing agents for EDOT are iron(III) chloride (FeCl₃) and iron(III) tosylate. The polymers generated by these oxidants are easily prepared and result in a well-controlled deposition of films achieving high-conductivity, high transparency and good mechanical properties [59,60]. The research concentrated on iron(III)-based oxidants stems from the limited solubility of EDOT in water in contrast to its miscibility with alcohols [30]. In 2004. Ha et al. performed a methodical study on a variety of such solvents (methanol, ethanol, n-butanol, 2-methoxy ethanol, pentanol, hexanol), in which the influence of these and several other individual processing components on resulting PEDOT films was considered [30]. The concentration of the monomer and oxidant (iron (III) toulenesulfonate (Fe(OTs)3 - Tos)) were varied in addition to that of imidazole (i.e. the rate-inhibitor). The results demonstrated the ability to suppress overdoping and reduce surface roughness (Fig. 3a). The highest PEDOT conductivity (at that time) was attained, 900 S/cm, while increasing film transparency, particularly important for display technologies [61-63]. Numerous studies followed, aimed at further increasing the electrical conductivity of chemically oxidized PEDOT. Successful approaches will be highlighted in Section 3.2.1.

The examples of chemical oxidative polymerization thus far involve non-aqueous solutions. As stated above, this constraint is related to the poor solubility of EDOT in water. A well-known method to circumvent the water-solubility issue, however, involves the use of PSS, the most promising PEDOT counterion to date. The following sections will shortly overview PEDOT:PSS as well as the (typically) aqueous chemical oxidative polymerization of PEDOT using biopolymer dopants.

2.1.2.1. PEDOT:PSS. Poly(3,4-ethylenedioxythiophene):poly(styrene sulfonate) (PEDOT:PSS) is often created through chemical oxidative polymerization and is the most practically successful conducting polymer (CP) to date. The result is an aqueous microdispersion (i.e. not completely miscible with water), which may be obtained commercially [64]. Distinctive properties contributing to the success of PEDOT:PSS include this commercial availability as well as straightforward processing by versatile deposition techniques. Polymer films formed from the aqueous micro-dispersion possess high electrical conductivity, high optical transparency in the visible light range, intrinsically high work function, and good chemical and physical stability in air [65]. Although extremely practical, the capability to tailor polymer properties on a synthesis level are limited. This emphasizes the importance of additives and process parameter control to tune PEDOT:PSS films. For example, the electronic and mechanical properties may be significantly enhanced through the utilization of additives such as organic (co)solvents, ionic liquids, surfactants, as well as thermal or acidic post-treatment methods [66-73]. These methods are often utilized in order to take full advantage of application-specific tailoring possibilities, enhancing substrate wettability, stability, flex/stretch performance, conductivity, and transparency. A substantial amount of work has been carried out related to this topic of PEDOT:PSS film modification and the resulting

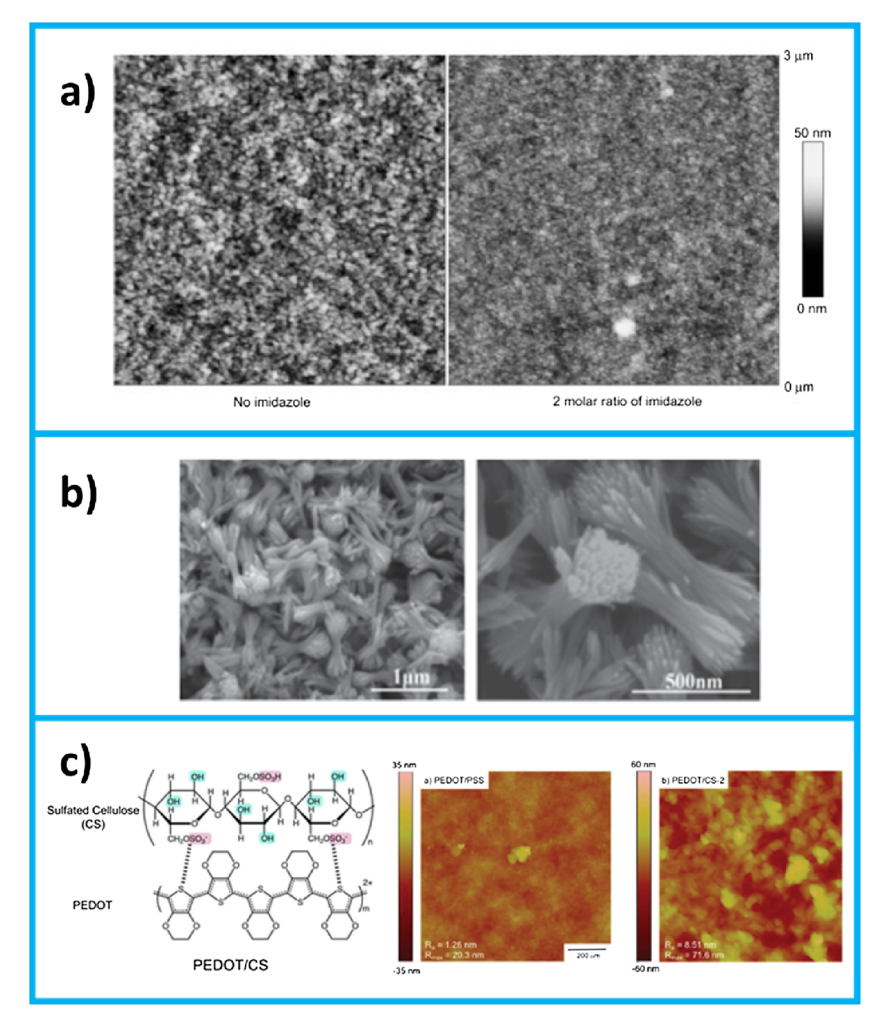


Fig. 3. Examples of chemical oxidative polymerization of PEDOT. **a)** AFM images of films polymerized using oxidant Fe (OTs)₃, demonstrating a decrease in surface roughness through the use of a polymerization rate inhibitor (imidazole), resulting in better transparency and simultaneous improvement in conductivity [30]. **b)**, **c)** Chemically polymerized PEDOT films with biopolymer counterions. **b)** PEDOT:hemin "brooms" [75] and **c)** PEDOT:sulfated cellulose chemical structure and AFM morphology comparison with PEDOT:PSS [79]. Blue borders group images from specific studies. Reproduced with permission of: [30,75,79] (For interpretation of the references to colour in this figure legend, the reader is referred to the web version of this article.).

mechanical and electrical properties. Conductivity improvement has received the most attention to date and the related accomplishments will be covered in Section 3.2.1, while adjustability of PEDOT:PSS mechanical properties is overviewed in Section 3.1.1 [32,64,73]. Finally, many of the bio-interfacing examples in the applications section (Section 4) employ this material, benefitting from the research carried out to tune the material properties.

2.1.2.2. PEDOT:Biopolymer. As pointed out in Section 2.1.1, biopolymer dopants are particularly interesting for naturally improving the interface with biological tissue. Driven by the motivation to enable use of PEDOT:biopolymer compounds on insulating substrates and to allow bulk production, chemical oxidative polymerization has been explored. An initial demonstration of this route was given in 2010 using DNA as the dopant/counterion, but relatively few examples are present in literature since this report [74]. The last few years, however, have revealed advancements in this area of research. Although not targeted specifically at bio-applications, interesting nano-structures were demonstrated by Guo et al. in 2014 through a study on the use of hemin as the counterion [75]. The resulting hemin-doped "PEDOT brooms" demonstrated good performance for non-precious-metal oxygen reduction reaction (ORR) catalysts (Fig. 3b). The following year, Harman et al. reported on a water dispersion using polysaccharide polyanion dextran sulfate (DS) [76]. The PEDOT:DS films were successfully deposited by drop casting, spray coating, inkjet printing, and extrusion printing. The cell line L-929 was used to investigate cytotoxicity, however through the addition of various concentrations of PEDOT:DS or PEDOT:PSS to the cell medium, opposed to the often employed technique of cell growth on the deposited polymer. This is likely due to the lack of stability in aqueous media as no stabilizing/crosslinking additive is utilized. In the cell medium/polymer dispersions, similar proliferation rates of the L-929 cells were observed for both PEDOT:DS and PEDOT:PSS in the initial 24 h, while after 4 days PEDOT:PSS demonstrated a 15 %-25 % lower proliferation rate when compared to PEDOT:DS and the control.

Recently, a study targeting sustainable energy applications utilized PEDOT:lignin, both electrodeposited and chemically polymerized, emphasizing the abundance of lignin available in nature [77]. While this study was not specifically aimed at improving a bioelectronic interface, relevant parameters, such as specific capacity of the electrode (important for recording and stimulation of biological signals) and electrochemical stability over time (essential to maintain functionality), are reported. A study by Mantione et al. in 2016 incorporated various GAGs into PEDOT films. Hyaluronic acid (HA), heparin, and chondroitin sulfate (CS) were used, and PEDOT:GAGs showed positive results regarding longer neurite outgrowth of differentiated SH-SY5Y cells in comparison to PEDOT:PSS [78]. Additionally, a neuroprotective characteristic of PEDOT:CS was suggested, demonstrated through better cell viability upon H₂O₂ exposure when compared to the other polymer complexes. The research focused on chemical oxidative polymerization

of PEDOT:biopolymer films will allow for facile deposition using common coating and printing methods, such as spin-coating, drop-casting, and inkjet printing. The electrical conductivity of drop- or spin-cast films to date, however, displays similar values to pristine PED-OT:PSS (between 10^{-1} -10 S/cm) and requires improvement. Horikawa et al. demonstrated an example of higher PEDOT:biopolymer conductivity through the utilization of sulfated cellulose as the counterion (Fig. 3c) [79]. A conductivity 38 times higher than pristine PEDOT:PSS, as well as better transparency (across the range of 200 nm–800 nm), was observed for an optimized degree (1.03) of substitution of sulfate groups on the cellulose. In order to extend the practical use of PED-OT:biopolymer compounds, this electrical conductivity, as well as the mechanical characteristics, of PEDOT:biomolecule dispersions must be further improved.

2.1.3. Vapor phase and chemical vapor polymerization

Vapor phase polymerization (VPP) and polymerization through chemical vapor deposition (CVD) may be viewed as subcategories of chemical oxidative polymerization. Both profit from what is often termed a 'dry' or solvent-less deposition, providing compatibility with insulating and/or complex surfaces, without dependence on wettability of the substrate (Fig. 4a,b) [80]. The polymerization process is induced chemically, requiring the use of an oxidizing agent. The main difference between VPP and CVD lies in the application of the oxidizing agent. In the case of VPP rather simple equipment may be utilized (i.e. lower vacuum levels or ambient pressure), however the oxidizing agent is typically deposited onto the substrate prior to vapor deposition of the monomer (an illustrative example set-up depicted in Fig. 1b). CVD, on the other hand, requires a controlled high-vacuum environment, but no liquid-based pretreatment steps are needed as the oxidizing agent is introduced as a vapor into the deposition chamber [81], [82]. VPP (of non-conducting polymers) was reported in 1978 by Cullis et al., and first demonstrated for CPs (by CVD) some years later by Mohammadi et al. using PPy [83], [84]. In 2003, Kim et al. were the first to successfully apply this technique to PEDOT attaining a conductivity of 70 S/cm [85]. Due to the complex nature of the process, intensive research has been carried out to accomplish deposition of various CPs and improve the resulting film properties. Additives may be employed to influence polymer properties, similar to the alternative polymerization processes; however, in this case they are applied to the initial oxidant or introduced into the reaction environment as a vapor along with the monomer. The use of pre-/post-treatment methods and variation of the counterion or process parameters may also be applied to VPP or CVD processes to tune the PEDOT film properties. In addition, the different vapor deposition processes also have a significant effect, as may be seen in Fig. 4c through the morphology comparison between CVD and VPP. In this example the focus was on the deposition technique while fixing all other parameters [86]. Typically employed VPP oxidant solutions are iron(III) tosylate or iron(III)Cl₃, however various sulphonate derivatives (trimethylbenzenesulfonate, iron(III) sulphonate), CuCl₂, Br₂

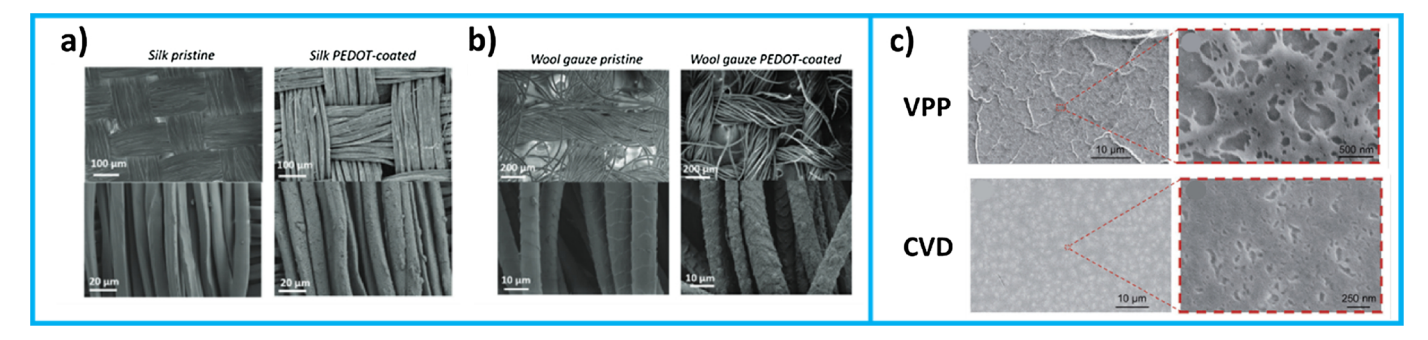


Fig. 4. VPP on complex insulating (a) silk and (b) wool gauze surfaces [80]. c) Comparison of morphology (shown here), ion transport, and electrochemical stability of PEDOT deposited by VPP and CVD employing the oxidant iron(III)Cl₃ [84]. Blue borders group images from specific studies.

Reproduced with permission of: [80,86] (For interpretation of the references to colour in this figure legend, the reader is referred to the web version of this article.).

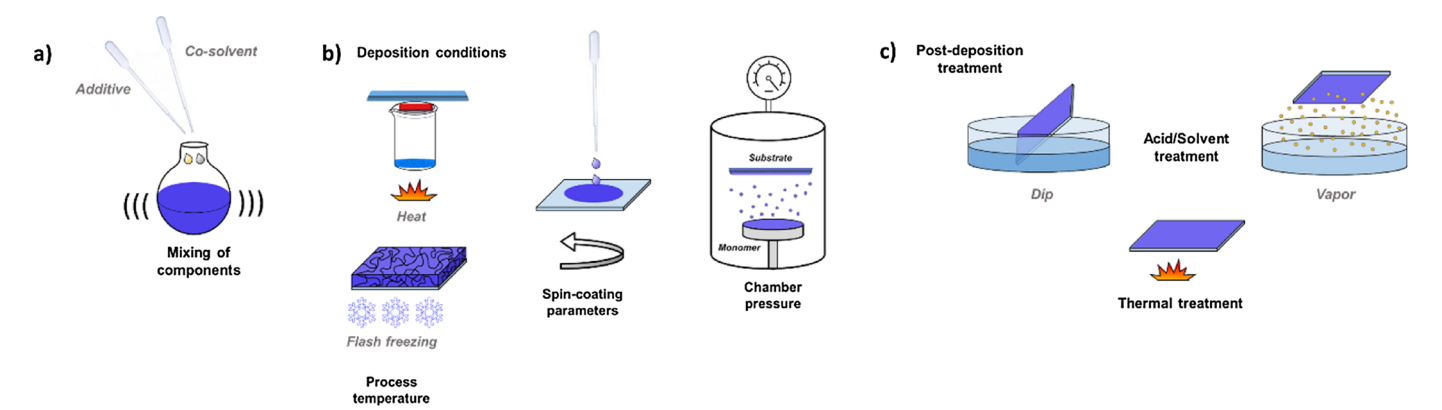


Fig. 5. Example methods to control and modify PEDOT film properties. a) Direct addition of additives or co-solvents to the polymer solution. b) Variation of deposition conditions, for example process temperature, flash freezing of deposited films, spin coating parameters, process pressure, etc. c) Post-deposition treatments, such as dip-treatment or exposure to the vapor of acids/solvents, or post-process thermal treatments.

and HAuCl₃ have also been used [58,87-90].

As a result of the controlled molecular growth of CVD/VPP processes, a great deal of research has been carried out to improve the conductivity of vapor phase deposited PEDOT. Specific examples of these will be discussed in Section 3.2.1; however, in general, reaction rate controlling additives and tuning process parameters to regulate the crystal growth have been extremely important [57,58,91,92]. Work on these topics, in addition to the use of small counterions to allow for small stacking distances between crystalline planes, have pushed films grown in the vapor phase growth to the highest reported conductivity value to date of all PEDOT polymerization methods (8800 S/cm) [93]. In order to compliment the conductivity achievements and to take full advantage of the compatibility of VPP/CVD with complex or insulating substrates, modification of mechanical properties must be further explored. Variation of additional characteristics such as mechanical flexibility and stretchability, ionic transport, and biocompatibility will enable the use of the advantageous properties of VPP/CVD films in the field of bioelectronics. An overview of the research to date aimed at enhancement of mechanical properties will also be discussed in Section 3. In general, further information may be found in the excellent overviews on VPP of PEDOT and other CP films from Lawal and Wallace, as well as Brooke et al. [94,95].

2.2. Summary

In summary, the utilized polymerization method and processing parameters significantly affect the resulting polymer film. Electrochemical and VPP methods typically provide a higher degree of freedom regarding polymer film adjustability, and result in valuable material properties such as high conductivity, surface quality, and stable redox chemistry. However, electrochemical polymerization is limited to conducting substrates. Therefore, to improve substrate variability as well as large-scale applications, vapor phase deposition or chemical oxidative polymerization processes are preferred. All methods possess the possibility to tune specific process parameters in order to tailor the characteristics of the resulting polymer. In addition, additives or co-polymers may be employed to modify the film properties. In the following sections, a variety of approaches will be highlighted, demonstrating the ability to modify PEDOT films in order to better match the diverse demands of individual applications.

3. Methods for improving the properties of PEDOT

The previous section focused mainly on variation of process parameters for the different polymerization methods. The resulting morphology variations as well as the achievements in conductivity enhancement are extremely useful, however, in order to fully take

advantage of PEDOT-based films for flexible or stretchable opto-electronic and bioelectronic applications, a variety of additional features must be considered. These include mechanical and electrochemical stability over time, biocompatibility, and ductility or Young's modulus. While developing methods to improve these characteristics, good conductivity of the material must be maintained. This section will review successful techniques to adapt film properties for specific applications and the following Section 4 will discuss selected bioelectronic applications benefiting from these approaches.

3.1. Mechanical properties

3.1.1. Mechanical stability and adhesion

An important attribute of PEDOT films is the mechanical stability, in particular for implantable devices, those used long-term on tissue surfaces (i.e. electronic skin), or *in vitro* platforms where days up to months stability in complex fluid environments is required. Mechanical stability to withstand bending or tensile strain as well as the adhesion of the PEDOT film to the substrate are clear points of importance to obtain useful bioelectronic devices, however not necessarily straightforward to accomplish. These topics are significant for all polymerization methods, with significant concern for long-term use of these materials in biological applications. In this section, we highlight methods that have been developed to increase this stability for the various polymerization techniques.

3.1.1.1. Electrochemical polymerization. Studies on the mechanical stability of electropolymerized films primarily focus on substrate adhesion as this is one of the main causes of failure for these films. A great deal of research has investigated conductive polymer coatings of clinical electrodes through electropolymerizaion to improve biological recording or stimulation performance. However, as these electrodes typically consist of inert metals, a covalent chemical bond to the conductive electrode is typically not made and upon use cracking and/ or delamination often occurs [12,22,96,97]. To improve the physical interaction between PEDOT films and the conductive substrate, and thus to improve interfacial adhesion properties, multiple approaches have been explored. In order to understand potential adhesion improvements, various methods are employed, ultrasonication, scotch tape, and cyclic voltammetry or other electrochemical stress testing. Each of these methods stress the deposited film in different ways. Further information on adhesion testing may be found in Tables 1 and 2 as well as by Qu et al. [145,150].

A simple surface roughening of the substrate prior to deposition has shown improvements in adhesion [97,98]. A study by Green et al. employed a laser treatment to create roughened Pt surfaces. In addition to substrate roughness, the effects of dopant chemistry were studied,

comparing pTS, ${\rm ClO_4}^-$, and PSS counterions under passive and active (stimulation) conditions. Electrodes with roughened surfaces and employing pTS or ${\rm ClO_4}^-$ withstood 1.3 billion cycles of biphasic stimulation, while PEDOT:PSS showed delamination and significant loss in charge storage capacity. This study additionally investigated polymer stability following sterilization processes, demonstrating good results – a crucial point of importance for long-term implantable bioelectronic applications. Pranti et al. also made use of a surface roughening approach through iodine etching of gold surfaces prior to PEDOT deposition [98]. This method provided films capable of withstanding 11 min of aggressive ultrasonication bath exposure with minimal increase in impedance, while non-etched gold delaminated after 5 – 7 min.

Various material combinations and nanomaterial techniques have been considered to improve the stability of electropolymerized conductive polymers [99]. For example, Abidian et al. created conducting polymer nanotubes through an electrospinning technique, depositing PLLA nanofibers and subsequently electropolymerizing the conducting polymer [100]. Following dissolution of the nanofiber scaffold, PEDOT or PPy nanotubes remain on the electrode surface and show improved adhesion when compared to the polymers deposited without this nanostructure. Although an interesting method regarding the increase in surfaces area, rather mild adhesion testing was carried out compared to other studies and, in addition, the films physically protrude from the substrate, potentially problematic for implantable devices. A study by Lu et al. employed poly(vinyl alcohol)/poly(acrylic acid) interpenetrating networks to increase adhesion and stability of PEDOT:PSS microwires on platinum electrodes for an in vivo optogenetics study [101]. In this work, the resulting interpenetrating PEDOT/PSS-PVA/ PAA networks demonstrated only 8 % loss in electrochemical performance following stability testing (100 CV cycles between -0.6 V and 0.6 V with a subsequent 1 week soak in ASCF), while PEDOT:PSS alone suffered 95 % loss. Boehler et al. investigated both surface structuring as well as chemical interaction at the polymer/metal (oxide) interface of PEDOT:PSS and PEDOT:Dex on Pt. nano-structured Pt. and Pt/IrOx surfaces [102]. Rigorous stability testing was carried out, with CV cycling up to 10,000 cycles (-0.6 V - 0.9 V) and aging in 60 $^{\circ}$ C PBS for more than 110 days. Nanostructured Pt improved performance, however sputtered IrOx coatings on Pt surface demonstrated the best performance, serving as an excellent adhesion promoter believed to stem from both mechanical and chemical bonding. This study represents the longest stable PEDOT performance thus far (measured in a non-biological environment). The use of carbon nanomaterials such as graphene and carbon nanotubes have also been explored to improve PEDOT stability [103-105]. CNT-doped PEDOT films on platinum electrode surfaces were demonstrated to be extremely stable by Luo et al. [103]. Long-term stimulation pulses and CVs resulted in minimal loss of PEDOT:CNT electrochemical performance, and the material additionally demonstrated good in vitro biocompatibility [103]. Following these results, this technique has been employed by Kozai et al. for chronic neural recordings (see Section 4.2.3), resulting in the longest in vivo recording period to date using PEDOT [104].

A final promising method of improving the interfacial adhesion of electropolymerized PEDOT coatings involves chemical modification of the substrate to allow for covalent binding between the polymer and the substrate. This is a useful approach; however, care must be taken to avoid creating an insulating layer at the interface and to maintain good electrical connection between the electrode and polymer coating. This method was investigated in conjunction with conductive polymer coatings as early as 1995 when Mekhalif et al. studied the effects of various alkythiol or aromatic thiol treatments of metal electrode surfaces [106]. Chemical treatment variables such as the molecular structure, chain length, and solvent were taken into account to understand the resulting changes in adhesion and electrical performance of the subsequently grown polybithiophene polymer. A different approach was used by Carli et al., with the chemical functionalization taking place on the monomer. Aminopropyl-triethoxysilane functionalized

EDOT (APTES-EDOT) showed enhanced PEDOT adhesion on FTO, demonstrated through increased robustness in scotch tape and ultrasonication testing when compared to non-functionalized PEDOT [107]. This improvement is a consequence of the covalent bonding at the polymer/conductive substrate, however surface hydroxyl groups are needed to allow for the binding with the silane group of APTES-PEDOT, thus this may not be employed on inert metal surfaces. A separate EDOT functionalization strategy developed by Wei et al. employed carboxylic acid functional groups (EDOT-acid), to deposit monolayers on ITO and stainless steel [108]. Improved stability was demonstrated in comparison to no use of the EDOT-acid monolayer; however, only ultrasonication characterization (5 min) was carried out and only on the ITO substrate. Ouvang et al. proposed a further option for EDOT functionalization through the use of an amethylamine-functionalized EDOT derivative (EDOT-NH₂) [109]. In this report, long-term ultrasonication was used (up to 1 h) as well as CV cycling to assess performance. The adhesion following sonication visually appeared very good, while some decrease in electrochemical performance was seen after 100-300 CV cycles (Fig. 6a). Finally, Chhin et al. recently demonstrated excellent stability using an electrochemically grafted (i.e. covalently bound) "home-made" diazonium salt to improve adhesion to platinum and PtIr surfaces. The electrochemical grafting was carried out at the electrode surface prior to electrochemical polymerization of PEDOT [110]. CV cycling (1000 cycles) as well as ultrasonication tests (5-15 min) were applied with outstanding stability results (Fig. 6b).

3.1.1.2. Chemical oxidative polymerization. PEDOT:PSS. Although one of the great benefits of PEDOT:PSS is its water solubility, methods to improve the mechanical stability are required, in particular for bioelectronics where the films are often utilized in aqueous environments. Additives, such as glycidyloxypropyl)trimethoxysilane (GOPs) and divinylsulfone (DVS), that enable physical crosslinking have shown the most potential thus far to alleviate stability issues (Fig. 6c) [78], [111–113]. The addition of a small amount of GOPs to the PEDOT:PSS microdispersion (often in the range of 1 % v/v) has been widely used for a number of years to attain mechanical stability. Håkansson et al. proposed an explanation on the mechanism of this stabilization. This is illustrated by the bonding of the methoxysilane group of the GOPs molecule to the glass substrate or to other molecules (Fig. 6d). Additionally, the SO₃ groups of PSS are expected to interact with the epoxy ring of GOPs. This results in a network providing physical stability, however it is well known that the conductivity and elasticity decrease with increasing GOPs concentration [113,114]. Alternative crosslinking methods have thus been sought after to attain highly stable films while maintaining electronic and mechanical performance. Initial results on the use of demonstrate good electrochemical stability for up to two months and higher conductivity when compared to GOPs [78]. An additional advantage of this approach lies in the possibility to anneal the PEDOT:PSS films at room temperature. Further work regarding crosslinking techniques will continue to be important to enable use of PEDOT:PSS for long term bioelectronics applications or for devices requiring extensive processing steps, where the PEDOT film comes into contact with an assortment of solvents.

The crosslinking agent may also aid in solving the issue of substrate adhesion, as stated above for the case of glass illustrated in Fig. 6d. In this example, the hydroxyl groups present at the glass substrate surface are essential. Surface treatments, such as $\rm O_2$ plasma, UV, or chemical (i.e. acid), may be employed to induce these surface groups, on substrates such as PDMS or PaC [21,115]. Alternatively, chemical coupling agents not requiring hydroxyl groups and compatible with the utilized substrate may be employed. For example, Curto et al. have demonstrated the importance of an adhesion promoting layer for spin cast films of PEDOT onto gold contacts. In this case the gold does not provide an opportunity to form a covalent bond to PEDOT:PSS or the discussed crosslinking agents (i.e. GOPS, DVS). However, through the

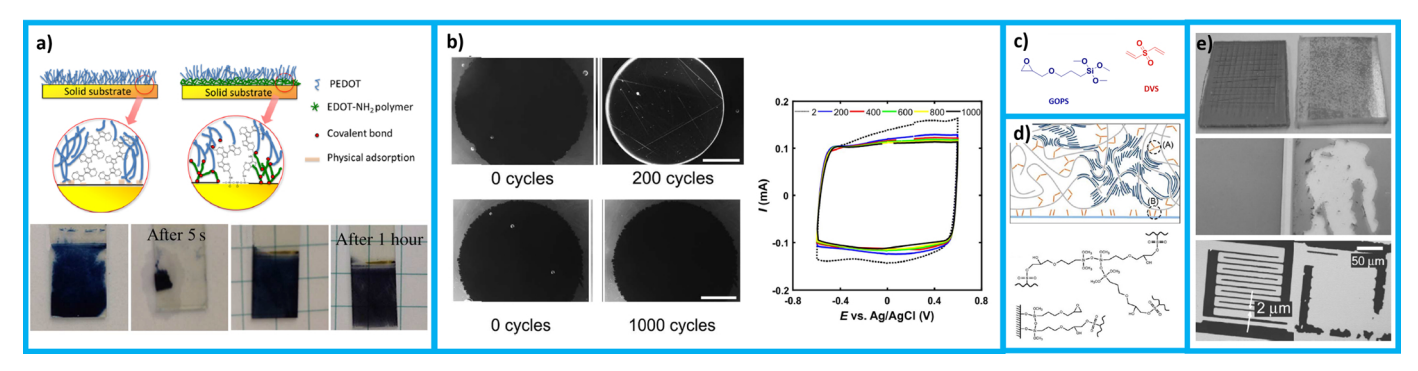


Fig. 6. Adhesion improvement of PEDOT films. a) Electrografted P(EDOT-NH2) on metal electrodes to act as an anchoring layer for subsequently electrodeposited PEDOT layers. Adhesion improvement is demonstrated through CV cycling and ultrasonication treatment (bottom) [109]. b) Grafting of a "home-made" diazonium salt onto Pt electrode surfaces to improve adhesion and electrochemical stability of the following polymerized EDOT layers [110] c) PEDOT:PSS crosslinker examples (glycidyloxypropyl)trimethoxysilane (GOPs) and divinylsulfone (DVS). d) Interaction of GOPS to crosslink the polymer as well as covalently bind to a glass substrate [112]. e) Adhesion improvement of oCVD films through grafting of the polymer to substrates with aromatic chemical structures. Top: Successful grafting on PET (aromatic), while unsuccessful on PP (non-aromatic) shown through tape/pull-off testing. Middle: Grafting of PEDOT on glass by chemical surface modification to include an additional linker molecule (phenyltrichlorosilane (PTCS)) provides stability for up to one hour of ultrasonication testing (left) while films delaminate after 5 min when PTCS is not used (right). Bottom: Chemical modification of Si substrates with grafting allows for micrometer-scale pattering of PEDOT using standard photolithography techniques (left), while delamination occurs when no linking molecule is used (right) [126]. Blue borders group images from specific studies. Reproduced with permission of: [109,110,112,126] (For interpretation of the references to colour in this figure legend, the reader is referred to the web version of this article.).

use of a self-assembled monolayer of 3-mercaptopropyltrimethoxysilane (MPTMS) the adhesion of PEDOT:PSS was significantly improved by the covalent bond of this layer between the gold surface (as a result of the thiol chemical group) and the GOPs included in the polymer formulation [116].

PEDOT:biopolymer. During the development of PEDOT:biopolymer composites, a variety of material parameters have been investigated in order to evaluate the performance of the polymer, including electrochemical stability, electrochromic properties, conductivity, morphology, and biocompatibility [76,77]. In several cases, the experimental conditions involve non-aqueous environments, allowing for characterization of the material, however not demonstrating usability at bioelectronic interfaces. Experiments in which the PEDOT:biopolymer complexes are utilized in an aqueous or biological environment have primarily examined methods to mechanically fortify the polymer through crosslinking chemicals, analogous to those employed for PEDOT:PSS. GOPS has been used to stabilize PEDOT:GAG dispersions for cytotoxicity tests [78] and DVS was added to PEDOT:xanthan gum scaffolds to support 3D cell culture [117]. This mechanical crosslinking should be straightforward to apply to further biopolymer counteranion options which have been studied, such as alginate, cellulose, gelatin, and guar gum, as well as those that will be developed in the future [118].

An interesting addition to the combination of PEDOT with a biopolymer counterion involves blending the polymeric mixture with a secondary non-conductive co-polymer. These hybrid systems provide the opportunity to benefit from the electroactivity of the conducting polymer while imparting softer, more elastic properties of the nonconducting polymer. A particular subcategory of this approach are materials, known as conducting polymer hydrogels, which contain a conductive polymer along with a cross-linked hydrophilic polymer with high water content. Valued properties include high mixed electronic and ionic conductivity and flexibility while maintaining mechanical integrity. Mawad et al. employed this approach, demonstrating a functionalization method to obtain PEDOT-COOH, which is subsequently copolymerized with acrylic acid (AA) in the presence of poly (ethylene glycol) diacrylate (PEG-DA) as the film cross-linker. The resulting electroactive hydrogel scaffold was suitable for biointerfacing, shown through use as hydrated 3D structures for cell adhesion, proliferation, and differentiation [119]. The compliant nature of such conducting polymer hydrogels render these materials promising for bioelectronic applications, however a main drawback involves water evaporation and the subsequent loss of the valuable mechanical and electrical properties. In order to overcome the poor stability of the hydrogels, del Agua et al. recently developed a conducting gel with long-term stability [120]. This material presents a unique combination of properties by combining the ionic conductivity and negligible vapor pressure of the ionic liquid (IL) BMIMCl with the electronic conductivity of PEDOT and the mechanical softness of the polysaccharide. Flexible freestanding films were obtained, combining the conductivity of PEDOT, the mechanical properties of the polysaccharide, and improved ionic properties of the IL. This is a promising approach, however again characterization was carried out in non-aqueous environments and requires a cross-linking method to allow use in bioelectronic applications.

3.1.1.3. VPP/CVD. As a result of the limited use of VPP/CVD PEDOT films for bioelectronics, much of the work to date investigating the mechanical stability of PEDOT deposited from the vapor phase targets applications such as flexible photovoltaic, organic solar cell, or supercapacitors. In addition, a great deal of the existing research makes use of pre-stretched, flexible, or structured surfaces, taking advantage of the substrate variability CVD/VPP deposition, however not focusing on the mechanical integrity of the film itself. The cases that do investigate the stability of the deposited film tend to characterize with bending/buckling tests (see Table 1). Skorenko et al. employed this method to demonstrate improved mechanical properties of PEDOT:Fe(PTS)3 when compared to ITO coated PET as well as PEDOT:PSS on PET films [121]. Various counterions and oxidants were investigated, as well as use of the alkaline reaction rate controller, pyridine. The VPP polymerized films with Fe(PTS)₃ and using pyridine outperformed ITO and PEDOT:PSS in mechanical bending tests, retaining the highest level of conductivity. An interesting study by Talemi et al. employed the triblock copolymer PEG-PPG-PEG dispersed within the oxidant solution to investigate improvement of the mechanical stability of VPP PEDOT. This approach was previously employed by Fabretto et al. in research exploring glycol-oxidant complexes as alternative reaction rate controlling additives to understand the overall effects [122-124]. Talemi et al. demonstrated that this copolymer improves the mechanical stability with the resulting PEDOT:glycol film showing good resistance values up to 35 % strain. A poly(vinylidene fluoride)-based flexible piezoelectric device

was developed, demonstrating the possibility to create wearable or biomedical energy harvesting devices.

Further mechanical stability studies on VPP/CVD of PEDOT focus on the issue of adhesion to the substrate [125]. A methodical study was carried out by Im et al. in 2007 to develop a grafting technique of PEDOT resulting in covalent binding to substrates which contain an aromatic chemical structure [126]. A wide variety of substrates were utilized including those with aromatic groups (polystyrene, polyethyleneterephthalate, polycarbonate, polyethylenenaphthalate, polyurethane, and poly(acrylonitrile-butadiene-styrene), as well as those without aromatic rings (polypropylene, polyethylene, polyetrafluoroethylene, polyethyleneoxide, glass, and Si). Chemical functionalization of non-aromatic substrate surfaces, using silane coupling agents to induce covalent binding, was also studied. The grafting technique demonstrated highly improved adhesion properties (Fig. 6e) and preservation of electrochemical properties following rigorous ultrasonication testing.

3.1.2. Stretchability/Elastic modulus

In the case of bendable or stretchable bioelectronic applications, not only high conductivity and flexibility of the conductive polymer film are required, but also good elasticity to allow for intimate contact of the electronic transducer with biological tissue. This goes hand in hand with the elastic modulus of the material system, where low Young's moduli are sought after to better match the softness of human tissue. A variety of approaches are highlighted in this section which simultaneously achieve good conductivity and stretchability/elastic modulus. Electrochemical polymerization methods are omitted as these are typically carried out on non-stretchable conductive substrates.

Polymer blends. One technique to attain highly flexible or stretchable CPs is the creation of polymer blends. This blending approach aims to combine the desired electronic and/or ionic conduction properties of the CP with the bendable or rubbery nature of a second polymer. In 2007. Hansen et al. employed this technique, blending PEDOT: Tos with polyurethane elastomer (PUR), achieving stretch performance of over 100 % while retaining reasonable conductivity (~100 S/cm) [127]. Advantages of their method include the straightforward preparation of the polymer blend as well as the solution processability, which allows deposition on a variety of substrates. This technique has been adopted in the group of Kai et al., with a recent study focused on the electrochromic properties of the PEDOT:pTS/PUR composite film for stretchable, wearable display applications [128]. The free-standing films are utilized in combination with a hydrogel, acting as a stretchable electrolyte reservoir, to construct a stretchable electrochromic display (Fig. 7a). Good performance was shown with insignificant degradation following 100 redox cycles of the free-standing film, as well as reversible color switching at 50 % elongation. The reported elastic moduli down to 13 MPa, measured by the tensile strain test with a freestanding film (Table 1), is also a significant accomplishment for the desired bioelectronic applications. Choong et al. have also made use of a composite system, blending PEDOT:PSS and PUD and coating PDMS substrates to create pressure sensors for electronic skin, further discussed in Section 4 [129]. Employing a similar concept, Maziz et al. have reported on an interesting microactuator application using an "interpenetrating polymer network" (IPN) [130]. Contrary to a polymer blend, an IPN consists of two (or more) separate polymer networks interlaced throughout one another [131]. In this work, PEG, PEDOT, and nitrile butadiene rubber (NBR) are brought together, each contributing to the desired ionic, electronic and mechanical properties, respectively. The resulting micropatterned 'electroactive polymer micromuscles' demonstrate improved performance compared to previous results and have potential in microactuator applications.

PEDOT:PSS. The elastic performance of PEDOT:PSS (and other CPs) has been enhanced through various methods, including the abovementioned polymer blends, patterning of serpentine contacts, CP deposition on pre-stretched substrates, micro- or nanostructuring, and/or

directing strain away from active components dispersed across an elastic matrix [132,133]. However, the ability to render a conductive film 'intrinsically stretchable' through blending with additional components (Fig. 5a) is far more practical and avoids complicated fabrication techniques. Many approaches based on additives or secondary doping to achieve improved tensile (i.e. Young's) modulus typically enhance either the stretchability or the conductivity, but rarely both simultaneously [21,132,134]. Additives which have played an important role in the endeavor to achieve optimal stretchability and conductivity include ionic compounds such as ionic liquids (ILs), anionic surfactants such as sodium dodecvl sulfonate (SDS), or dodecvl benzene sulfonic acid (DBSA), and nonionic surfactant polymers polyethylene glycol (PEG). Zonyl (now Capstone), and p-t-octylophenol (Triton X-100) [6,66,72,135-137]. Following substantial work in this field over the past decades, major advancements have been reported in the past few years.

The effects of Zonyl fluorosurfactant and DMSO were investigated in 2015 by Savagtrup et al. to optimize the tensile modulus of PEDOT:PSS and increase resistance to film cracking [21]. Improved mechanical compliance was demonstrated for increased concentrations of Zonyl, subsequently utilized for skin-like resistive strain sensors, an application highlighted in Section 4. The following year Oh et al. reported on a "polymer dough" using the nonvolatile surfactant plasticizer Triton (Fig. 7b) [5]. With this additive alone the PEDOT:PSS films attained modest conductivity of approximately 80 S/cm; however, when coated over metallic circuits, a healing effect was observed with the PEDOT:PSS dough curing cracks in the metal upon applied strain, maintaining metallic conductivity.

Recent impressive results yielding highly stretchable and conductive PEDOT:PSS layers employ ionic additives such as ILs. In 2002, Lu et al. were one of the first to investigate the idea of IL additives in CPs, improving the long term electrochemical stability [138]. Some years later, Döbbelin, et al. applied this idea to PEDOT:PSS using a family of additives based on ILs, enhancing the charge transport the films with a factor of 500 conductivity increase [72]. This report also confirmed the presence of the ILs in the final polymer film. In 2012, Badre, et al. employed the IL 1-ethyl-3-methylimidazolium tetracyanoborate (EMIM TCB) to attain higher conductivities, up to 2084 S/ cm, with 96 % transmittance at 550 nm and good flexibility, however no analysis of elasticity [66]. Attaining good stretchability with conductivities in this range was first shown by Teo et al., using the same IL additive, EMIM TCB. Conductivity values greater than 1000 S/cm were achieved and maintained when the films were stretched up to 50 % on PDMS substrates and up to 180 % when deposition on a pre-strained substrate [132]. The following year, a remarkable achievement was reported in 2017 by Wang et al. in an investigation of an extended set of ionic compounds. Conductivities higher than 4100 S/cm under 100 % strain were achieved, in addition to record breaking strain performance of up to 800 % (Fig. 7c) [133]. The best performing ILs are understood to soften the PSS domains, while simultaneously promoting connectivity and crystallinity of PEDOT-rich regions, as illustrated in the left-hand side of Fig. 7c. This morphology enables both high conductivity and enhanced elastic performance (Fig. 7c, right), with Young's modulus values as low as 28 MPa [139].

3.1.2.1. VPP/CVD. Modification of the mechanical properties is essential for VPP/CVD of PEDOT films in order to take full advantage of the possibility to coat complex or insulating substrates. Only a few examples exist to date that have aimed at improving the elasticity of VPP PEDOT, where advancement has primarily been achieved through the use of co-polymer additives and hybrid-systems. Interestingly, Lamont et al. employed an elastomer designed for biodegradability, poly(glycerol sabecate) (PSG), to achieve a hybrid network with good response up to 25 % strain. PSG was impregnated with the oxidant solution (butanol) and VPP was subsequently carried out, creating a PEDOT network throughout the film [140]. In 2017, Boubee de

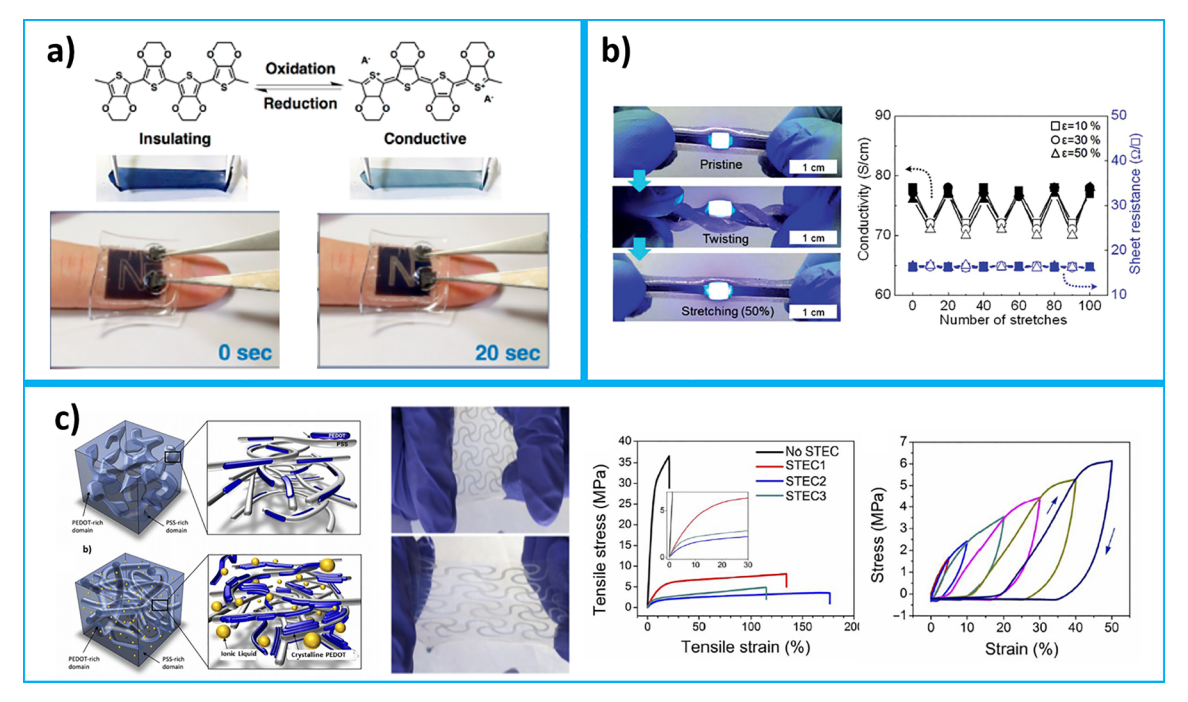


Fig. 7. Stretch performance of PEDOT films. a) A PEDOT:pTS/PUR blend for stretchable, wearable electrochromic display applications [128]. b) "Polymer dough" obtained through the use of additive Triton in a PEDOT:PSS formulation [5]. c) Schematic diagram representing the structure of a PEDOT:PSS film without (left, upper) and with (left lower) ionic liquid. Middle: Free-standing PEDOT:PSS/ionic liquid film with applied strain. Right: Stress-strain and strain cycling characterization curves [133]. Blue borders group images from specific studies.

Reproduced with permission of: [128,5,133] (For interpretation of the references to colour in this figure legend, the reader is referred to the web version of this article.).

Gramont et al. reported the highest stretchability achieved by vapor phase polymerized PEDOT to date [141]. This was accomplished using electrospun fibers containing a carrier polymer, polyvinylpyrrolidone (PVP), with iron(III)Tos oxidant and imidazole reaction inhibitor. The fibers were spun onto a PDMS substrate and followed by VPP, resulting in stretch performance up to 140 % while retaining conductivity.

In order to quantify and compare the stretch performance, as well as the mechanical performance in general, appropriate characterization techniques must be employed. Tables 1 and 2 give an overview of available techniques, many of which are utilized to obtain the discussed results.

3.2. Electronic/electrochemical properties

3.2.1. Conductivity

Although the conductivity of the various PEDOT-based films is a topic that has come up briefly in other sections, here we overview the most successful methods for achieving improvement of this property. Good conductivity is important to most bioelectronic devices and must be maintained while adjusting other material parameters for application-based optimization.

3.2.1.1. Electropolymerization. Measurement of the conductivity of electropolymerized PEDOT films is not straightforward, as the deposition takes place on a conductive substrate. Typical characterization techniques such as two- or four-point probe measurements, which are made by placing the two or four electrodes onto the polymer film to be evaluated, give erroneous values due to the underlying conductive substrate. One technique to bypass this obstacle and allow quantification of electropolymerized PEDOT conductivities includes the construction of two (or more) band electrodes separated by micrometer-scale-thick insulators and subsequent polymerization until the electrodes are "bridged" by the conductive film (Fig. 8a, b) [36,151–153]. A secondary method involves polymerization within

the micrometer- and nanometer-scale diameter holes of microfiltration membranes. Conductivity measurement of the polymer within the pores is then made by contacting each side with gold electrodes and applying pressure [154].

Through use of the microfiltration membrane technique, Granström et al. demonstrated that the conductivity of geometrically restricted polymerization has a strong dependence on the pore size. This work investigated a variety of conducting polymers, and the use of PEDOT:ClO₄ in the smallest pores (10 nm) resulted in the highest conductivity 780 S cm $^{-1}$ [154]. Aubert et al. looked into a wider assortment of counterions, as well as employing both EDOT and EDOT- $\rm C_{14}$ monomers. The importance of an optimized oxidation potential was emphasized and ClO₄- also demonstrated the highest conductivities in this study, reaching 400 S cm $^{-1}$ for PEDOT and 1100 S cm $^{-1}$ for PEDOT- $\rm C_{14}$ [36]. To our knowledge, this result from 2002 is the highest reported conductivity to date for electropolymerized PEDOT. This is a result of the complex experimental set-up and, in particular for bioelectronic applications, the use of electrochemical impedance as a figure of merit when comparing materials and processes.

3.2.1.2. Chemical oxidative polymerization. Intuitively, one would not expect an increase in conductivity through the addition of insulating components. This type of additive or secondary dopant has proven to be extremely important, however, for chemically oxidized PEDOT. In Section 2.1.2 attention is brought to the study of Ha et al., in which monomer, oxidant, reaction rate controller (Im), solvent and solution concentrations are systematically varied. A conductivity of 750 S/cm (84 % transparency) was achieved using 60 % pentanol solution and a 2:1.75:1 ratio of Im/Fe(OTs)₃/EDOT, while a methanol-substituted derivative of the monomer demonstrated 900 S/cm (82 % transparency) when using 60 % methanol solution and a 2.5:2:1 ratio of Im/Fe(OTs)₃/EDOT – CH₂OH. In 2013, Park et al. investigated various reactivity-inhibitors in solution casted films, aiming towards energy generation applications. Optimized processing conditions were

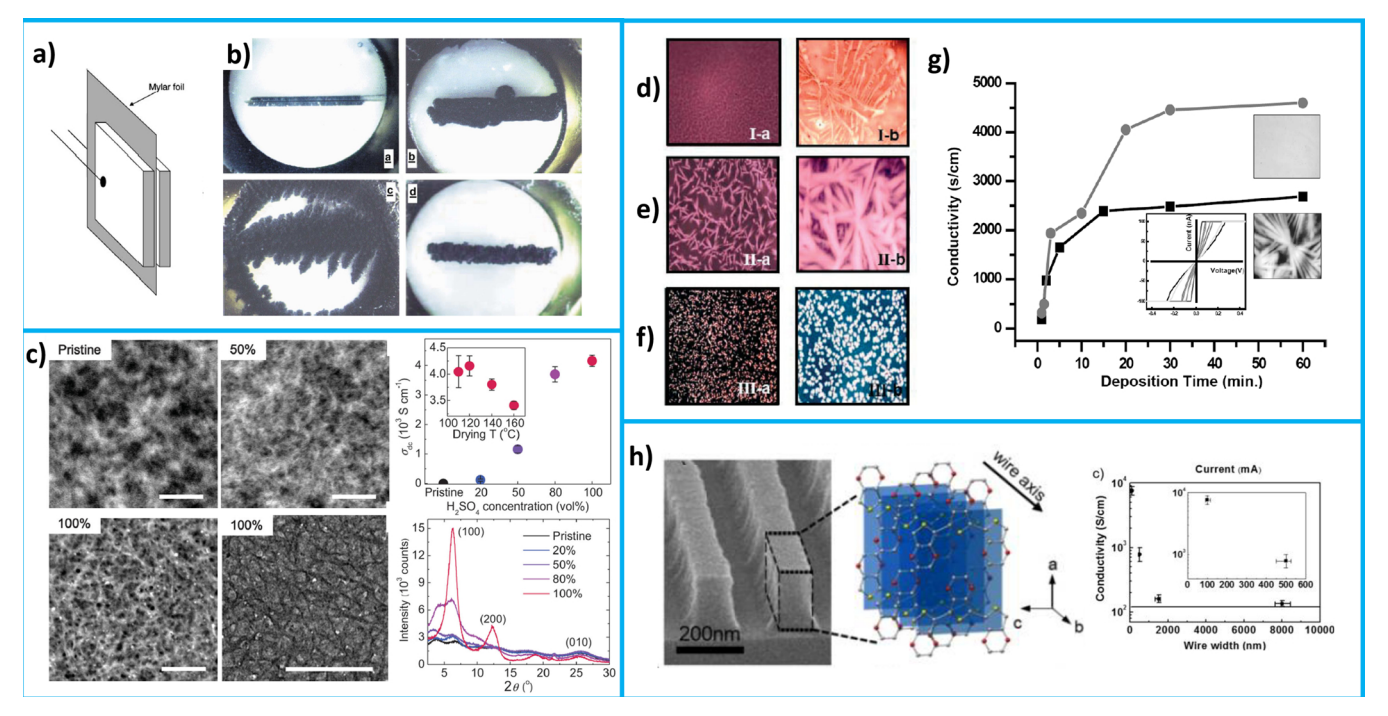


Fig. 8. a) Experimental setup enabling conductivity measurements of electrochemically polymerized films using two electrodes separated by a thin insulating layer. **b)** Optical images showing the increasing polymerization times to bridge the gap between the closely spaced electrodes [36]. **c) Left:** HAADF-STEM images of H₂SO₄ post-treatment on PEDOT:PSS films utilizing various concentrations (indicated in percentages). **Right:** Resulting conductivity increase and XRD patterns demonstrating improved crystallinity as a function of H₂SO₄ concentration [70]. **d)-g)** Effect of polymerization temperature on the conductivity of VPP of PEDOT employing pyridine rate-controller and using the oxidant iron(III) tosylate at (d) 15 °C, (e) 40 °C, and (f) 80 °C, and (g) the resulting conductivity [91]. **h)** High conductivity PEDOT nanowires formed through nanotransfer printing of the oxidant iron(III)Cl₃ and a subsequent VPP process [93]. Blue borders group images from specific studies.

Reproduced with permission of: [36,70,91,93] (For interpretation of the references to colour in this figure legend, the reader is referred to the web version of this article.).

found for oxidant solutions containing both PEG-PPG-PEG and pyridine. This resulted in good control of the polymer oxidation level, generating conductivities up to 1355 S/cm and a high thermoelectric power factor of 1270 $\mu\text{W/m}\ K^2$ [60]. Resulting films were employed on flexible substrates in a demonstration of electricity generation using human body heat.

The highest chemically polymerized PEDOT film conductivity to date was demonstrated in a recent investigation on utilization of the high boiling point co-solvent, N-Methyl- 2-pyrrolidone (NMP) on PEDOT films with small counter-ions [56]. Gueye et al. attained conductivities up to 5400 S/cm, through 'dopant engineering' of films based on trifluoromethanesulfonate CF₃SO₃ (PEDOT:OTf), carried out through optimization of the NMP co-solvent concentration, reaction rate controller, and sulfuric acid post-treatment. The authors show a combination of amorphous and crystallite regions present and hypothesize that the increase in conductivity resulted from the increase of mean crystallite size. Although the improvement in performance in this study is impressive, the extreme order in three dimensions shown is not typically observed or expected for PEDOT and is a point that should be further investigated [155]. Proposed applications include the often sought after ITO-alternative for flexible organic photovoltaic devices [7,59,134].

PEDOT:PSS. A great deal of work has gone into increasing the conductivity of chemically oxidized, commercially available PEDOT:PSS from its value of ~ 1 mS in the pristine state [70,73,156,157]. An early study by Kim et al. in 2002 demonstrated the effect of secondary solvent variation on the conductivity of PEDOT:PSS. Organic solvents including dimethyl sulfoxide (DMSO), N,N-dimethyl formamide (DMF), tetrahydrofuran (THF), and H_2O were added in varying concentrations to PEDOT:PSS solutions, which were subsequently spin coated. The PEDOT:PSS chain conformation and the

doping concentration of the film are understood to be unchanged for the various solvents, while an improvement in conductivity is observed, increasing two orders of magnitude in the case of DMSO (from 0.8 S/cm to 80 S/cm) [59,158]. This enhancement was presumed to be a screening effect between the dopant and the polymer main chain. This presumption was questioned in a study by Louwet et al. the following year where no ordering of the polymer film was observed when using the high boiling point solvent NMP to attain increased conductivity [159]. Following these initial studies, a great deal of work has gone into improving the conductivity of PEDOT:PSS and understanding the mechanism behind this increase, through the use of additional polar organic solvents (EG, glycerol, sorbitol, methoxyethanol, diethylene glycol, dimethyl sulfate, meso-erythritol, xylitol) [37,65,72], [92,160–164]. Further propositions on the mechanism of conductivity enhancement include Pettersson et al. suggesting the reorientation of polymers chains by a plasticizing effect (using sorbitol) and Ouyang et al. on conformation changes of PEDOT chains to more linear or expanded coil arrangements (using EG, among others) [69,165]. Indeed a great deal of evidence has now been given for conformational changes based on phase separation of PEDOT and PSS regions. A report by Nevrela et al. in 2015 carefully studied these effects based on four selected polar organic compounds (DMSO, EG, DMF, sorbitol) [163]. Emphasis was given to clarify previous false hypotheses on charge transport enhancement as well as to demonstrate the "secondary doping" or co-solvent role of the additives, i.e. influencing film properties, however not present in the final film [156]. Via careful processing techniques a conductivity increase of approximately three orders of magnitude (to 765 S/cm) was achieved, with a nearly identical effect of all four secondary dopants [163]. Raman spectroscopy and the variable range hopping model for charge transport were employed to confirm a three-dimensional hopping behavior, resulting from phase transition of

Table 3Overview of polymerization properties and important parameter optimization.

	Electrochemical polymerization	Chemical polymerization	Vapor phase polymerization			
Oxidant agent Type of counterion	External potential ClO ₄ ⁻ , Tos ⁻ , PF ₆ ⁻ , SO ₄ ⁻ , PSS, poly(B-hydroxyethers) (S-PHE)	$Fe(III) \ salts, \ (NH_4)_2S_2O_8, (Na)_2S_2O_8$ Often large counterions: PSS, biopolymers	Fe(III) salts, typically iron(III) tosylate Small counterions: Cl ⁻ , Tos ⁻			
Advantages	Electrochemical/film properties. Variety of counterions	Substrate variation (i.e. both conductive and non- conducting). Straightforward additive or polymer blend possibility.	Highest electrical conductivity. Good transparency. Substrate variability (including complex insulating surfaces)			
Application	Polymer film electrodes	Large-scale applications	Conductive film on flexible and rigid substrates			
	Conductivity					
Top performer(s) Method	780 S cm ⁻¹ [154] 1100 S cm ⁻¹ [36] ClO ₄ ⁻ , polymer nanofibers created through polymerization within micro-pores [154] EDOT-C ₁₄ monomer, ClO ₄ ⁻ [36]	5400 S cm $^{-1}$ [56] PEDOT:OTf / NMP and $\rm H_2SO_4$ treatment	8800 S cm ⁻¹ [93] FeCl ₃ , structuring through printing to achieve nanowires			
	Stretchability					
Top performer(s)	-	Max: 800 % [133] 4100 S/cm at 100%	140 % [141] ~100 μA over 50 cycles of 100% strain***			
Method	-	PEDOT:PSS with IL additives	Electrospun fibers / carrier polymer (PVP) with iron(III)Tos oxidant / imidazole reaction inhibitor			
	Transparency*					
Top performer(s)	-	> 80 % [30] with $\sigma = 900 \text{ S cm}^{-1} 82\%$ ** [176] R_s of 46 Ω \square ⁻¹ Stretchability of 10%	> 80 % [177] with σ = 3400 S cm ⁻¹			
Method	-	Fe(OTs) ₃ , Imidazole, Methanol, EDOT-CH ₂ OH monomer [30] PEDOT:PSS, Zonyl [176]	Fe(III) tosylate, PEG-PPG-PEG block co- polymer			
	Young's Modulus					
Top performer(s) Method	40 MPa [178] PEDOT:pTS, hydrogel (PVA-HepMA and 30HepMA) deposition, further polymerization through hydrogel	28 MPa [133] 13 MPa [128] 47-80 kPa [179] PEDOT:PSS with IL additives [133], PEDOT/PU film with 20% PEDOT content [128], PEDOT:PSS- PAAm organogels [179]	-			

^{*} Visible spectrum.

the films creating molecular crystal phases. Donoval et al. corroborated this lack of dependence on secondary dopants in a study using the same four solvents and observing very similar maximum conductivities. Additionally, further evidence was provided on the phase separation of PSS-rich islands, increasing with (secondary) dopant concentration [166]. This conductivity range was also demonstrated by Kim, et al. in 2011 using EG, however by employing an additional EG post-treatment bath for 30 min, the measured values nearly doubled, up to 1418 S/cm [245].

Post-treatment methods have also been employed using other compounds such as alcohols and strong acids [69,167,168]. Xia et al. utilized an amphiphilic germinal diol, hexafluoroacetone, applied by drop casting onto a heated PEDOT:PSS film to attain a conductivity of over 1000 S/cm [168]. A dual step DMSO post-treatment, applied as a vapor and subsequent immersion in a bath, was reported by Yeo et al. with performance up to 1475 S/cm [169]. Employing only a strong acid post-treatment, Kim et al. have reported the highest PEDOT:PSS conductivity to date reaching a value of 4380 S cm $^{-1}$. Immersion in sulfuric acid (H₂SO₄) resulted in the often-reported phase segregation and a clear removal of insulting PSS from the film (Fig. 8c) [70]. The drying temperature was also found to significantly influence the results.

3.2.1.3. VPP/CVD. Conductivity enhancement of VPP/CVD of PEDOT has primarily been achieved through control over the polymerization reaction through temperature control and the use of chemical additives. In 2004, Winther-Jensen utilized an organic alkaline additive, pyridine, to investigate and modulate the influence of pH on EDOT polymerization. A significantly higher conductivity compared to

previous results (over 1000 S/cm) was achieved by controlling the acidity and avoiding unwanted acid-initiated side reactions [57,58]. This use of alkaline rate inhibitors was further explored by Kim et al. in 2007 reaching a conductivity value of 4500 S/cm while also achieving ~90 % transparency [91]. In this work, an investigation of different counterions (ToS vs Cl) and the effects of temperature variation during VPP was carried out, with various ensuing polycrystalline structures, highly dependent on chamber temperature (Fig. 8d-g) [91]. Through careful control of process parameters and suppression of crystal growth, high-quality PEDOT films were prepared on flexible substrates with conductivity/transparency performance analogous to ITO. The same year, Im et al. further demonstrated the importance of temperature during CVD using iron(III)Cl₃, with resulting conductivities over a range of five orders of magnitude and demonstration of work function control from 5.1 to 5.4 eV [92,170]. Over the following five years, several groups carried out studies to more precisely understand the effects and limitations of alkaline or amphiphilic copolymer additives, the presence of water (i.e. the relative humidity during reaction), and the growth mechanism of the process as the monomer reaches the substrate [89,122,171–174]. Evidence for "bottom up" polymer growth has been given and this understanding along with additive/parameter optimization has led to reproducible, smooth, and highly conductive films, mainly for opto-electronic applications. Recently, the highest PEDOT conductivity values to date have been reported by Cho et al. (on average 7800 S/cm, up to 8800 S/cm) [93]. In this example, the small Cl counterion was again employed in a selective printing process of the iron(III)Cl₃ oxidant with a polyurethane acrylate (PUA) mold, enabling the formation of monocrystalline PEDOT nanowires

^{** 550} nm.

^{***} Conductivity values not extracted due to difficulty measuring film thickness.

(Fig. 8h). The use of these nano-structures allowed for the advantage of a compact PEDOT:Cl film with the smallest reported $\pi\text{-}\pi$ stacking distance and high carrier mobility (up to 88 cm²/V-s), while avoiding negative crystal formation effects observed in previous studies using iron(III)Cl₃ [91,175]. Field effect transistors (FETs) were fabricated on a transparent, flexible substrate taking advantage of the single-crystal PEDOT nanowires as flexible electrodes [93]. In general, the excellent electrical performance of vapor-deposited PEDOT is a result of the consecutive stacking of individual monomers as they reach the substrate. This enables a highly ordered polymer and a resulting crystalline nature of the film [89,95].

3.3. Summary

In summary, additives and processing parameters significantly affect the resulting polymer film. Variation of these parameters may be used to optimize PEDOT and CPs in general for specific applications. An overview of the polymerization processes in general are given in Table 3 along with the most influential investigations and impressive results. Here the best performers in various categories and for the different polymerization processes are given. In the following section, selected bioelectronic applications making use of these advancements are discussed.

4. Applications

In this section, we highlight research in the field of bioelectronics that has benefited from the tunable nature of PEDOT. Many examples make use of adjustments affecting the mechanical properties, which improve conformability, flexibility, and stretchability for applications at the interface of biology and electronics. In general, these devices and materials fall into two categories depending on where they are applied: 1) non-invasive, including non-implantable wearable devices for a variety of physiological sensor applications and 2) invasive, including systems used to build *in vitro* tissue models, and implantable devices for *in vivo* applications.

4.1. Wearable bioelectronic devices

Sensors applied directly onto the skin or those patterned on textiles aim to record electrophysiological signals, changes in temperature, hydration, pressure/strain levels, and a variety of biochemical species (such as ions, proteins, metabolites, oxygen) in real time. Advancement of conformable sensors mounted onto the skin, integrated into textiles, or developed further to integrate with soft robotics will revolutionize diagnostics and healthcare [2,14]. The translation of these devices to daily life depends largely on the mechanical compatibility, durability, and processability of the conducting material.

4.1.1. Strain sensors

Continuous monitoring of strain values is important in order to quantify body movements for medical assessment of muscles during sports, rehabilitation, and for injury prevention [180]. The use of PEDOT has aided in the advancement of this type of sensor. Reported results include not only reversible changes in the electrical properties (capacitance or resistance) upon mechanical deformation due to elongation and bending, but also the ability to endure repeated strain cycles. Improvement of the viscoelasticity is essential for this application field, which has been achieved by Lipomi et al. employing pre-stretched PDMS substrates. In order to maintain good conductivity and to provide wettability on the hydrophilic PDMS, PEDOT:PSS was blended with a nonionic surfactant (i.e. Zonyl) and DMSO [134]. Savagtrup et al. further investigated the effects of the Zonyl/DMSO ratio on the mechanical and electrical properties, and applied this to a wearable electronic sensor capable of measuring resistance variation as a function of bending strain [21]. The optimized film was coated on a PDMS substrate and attached to a glove, acting as a gauge to predict the maximum strain associated with the bending and unbending of the fingers (Fig. 9a). The Zonyl/DMSO-modified PEDOT:PSS film endured repeated deformation of 20 % strain. The capability to register the variation of resistance as a result of elastic deformation each time is a result of the attained mechanical robustness. This type of plasticized PEDOT:PSS could prove valuable in providing electronic feedback for medical prosthetics.

4.1.2. Pressure sensors

Whereas strain sensors detect lateral (tensile) strain, pressure sensors aim to sense the magnitude of force acting vertically on a plane (compressive strain) [139]. When applied to bioelectronics, the sensor requirements are increasingly complicated as good stretchability is also necessary. To provide the low mechanical modulus required by these applications, organic materials are often employed [13]. Common stretchable pressure sensor approaches involve microstructures and multi-material stacks to achieve piezoresistive, piezoelectric, triboelectric, or capacitive response [181-183]. These techniques aim to improve sensitivity to low-pressure modulation for health diagnostic or electronic skin applications. PEDOT is an ideal candidate for contributing to the advancement of this field, in particular when taking advantage of the possibility to modulate the stretchability and flexibility. Choong et al. demonstrated this through a blend of the polymer with an aqueous PU dispersion, thus endowing PEDOT with mechanical properties that enable its use as a piezoresistive electrode [129]. The peak stretchability performance was shown for 86 % PU in the composition, achieving up to 100 % strain with no cracks produced in the film. Making use of the Zonyl/DMSO additive ratio discussed above for strain sensors [21,134,176], sufficient conductivity was maintained for use as an electrode (ca. 50 S/cm). The piezoresistive effect was realized by coating the PEDOT:PSS/PU composite on top of a micro-pyramid PDMS array with spring-like compressible platforms (Fig. 9b), the microstructures used to increase the pressure sensitivity [129,181,184]. With these structures, the tip of the conducting pyramid spreads laterally upon application of pressure, resulting in modulation of the conductivity due to changes at the electrode interface. The good sensitivity was applied to a subject's wrist on a non-invasive bandage. Successful monitoring of blood pressure with high temporal resolution utilizing the micro-pyramid array was achieved.

4.1.3. Temperature sensors

Biological temperature changes may indicate a variety of diseases, muscle movements, and the healing of wounds [185]. As a result, stretchable temperature sensors that can be mounted on the skin have attracted attention in bioelectronics. Thermistors, or resistive temperature detectors, are often utilized, taking advantage of the principle that the resistance of a conductor varies with temperature. For application to skin, wavy metal lines have commonly been used, sandwiched between intrinsically stretchable substrates [186,187]. Trung et al. sought to avoid complicated fabrication processes through the development of a device fully composed of intrinsically stretchable materials, which also achieves high transparency. Various composites were employed to modulate the material properties, creating a transparent and stretchable resistive organic temperature sensor. This study was additionally extended to a transistor layout, capable of temperature and strain sensing by material modulation [191]. Once again taking advantage of the elastic properties of PU (as the example for stretchable pressure sensors), the fabricated transistor temperature sensor consists of a stretchable PEDOT:PSS/PU composite as the source, drain, and gate, a PU gate dielectric, and a reduced graphene oxide (rGO) nanosheet/PU composite temperature-sensitive channel [191]. The resulting structure exhibited stretchability up to 70 % as well as maintaining its response after 10,000 stretching cycles to 30 % strain. High temperature sensitivity of the transistor was achieved with $\sim 1.3~\%$ resistance change per °C, whereas the thermistor counterpart using the same temperature sensitive material exhibited 0.9 %/°C. Biological application was demonstrated by adhering transistor arrays to the skin using a patch, capable of minute temperature change detection, as small as 0.2 °C. In addition, strain sensors were realized exchanging Ag nanowires for rGO in the same transistor layout with the PEDOT:PSS/PU composite. These were mounted on the neck or arm of a test subject, allowing for simultaneous detection of temperature changes and muscle movements during sport activity or while drinking hot water. This work represents an example of the promising advancement toward all organic-based "electronic skin" or sensors for soft robotics.

4.2. Sensors of electrophysiological signals

The electrical activity of a biological system, such as an organ or tissue, is one representative measure of the physiological state of the system. For example, clinical monitoring of electrophysiological signals to identify a particular pattern can be used to detect a specific pathological state [192]. In general, when mounted on certain parts of the body, electrophysiological recording devices employing electrodes or transistors can monitor a variety of biological systems, including the cardiac cycle (electrocardiography, ECG), eye movement (electrooculography, EOG), or neurological rhythms (electroencephalography, EEG). The quality of these recordings is largely governed by the magnitude of the electrochemical impedance (discussed briefly in Section 2.1.1) at the electronic/skin interface. Due to the mixed ionic/electronic conduction and the resulting inherently low electrochemical impedance of PEDOT, electrodes made of this material show very good recording quality. Applications with electrodes fabricated photolithographically on flexible polyimide or more compliant parylene substrates have been reported to measure EEG signals [188,193], while a few of PEDOT electrodes printed on paper [194] or textiles [189,195-198] have successfully recorded ECG signals (Fig. 9c, d). For instance, ink-jet printed PEDOT electrodes provided high-quality ECG recordings, resistant to deformation. The reported conductivity of the electrodes remained constant withstanding more than 2000 cycles of bending [194]. As the electrodes are metal-free, an additional advantage of straightforward device recycling could be envisioned [158]. An important aspect of the production of these devices involves modulation of the viscosity to attain optimized printing of the film. Bihar et al. achieve good printability through the use of surfactants in addition to the utilization of GOPs to stabilize the polymer. Optimized inks reduce the rigidity of printed films and increase compatibility with nonlinear substrates such as paper or textile. The use of PEDOT-based electrodes has also demonstrated great potential for recording brain signals with implantable devices [43,199-201]. A focused discussion of implantable applications will be given Section 3.2.3, while the following two sections will review various PEDOT modifications aimed at improving soft actuators or in vitro tissue scaffolds.

Before moving on to these fields, a promising technology to further improve biological recording quality must be introduced. Organic electrochemical transistors (OECTs) are amplifying transducers ideal for bioelectronic applications as they translate fluctuations in the ionic potential of the biological media into an electrical signal, i.e., a change in the transistor drain current. The figure of merit is the transconductance, which defines the signal amplification and which was shown to be record-high when compared to other transistor technologies [202,203]. To date the OECT has most often been studied using PED-OT:PSS films optimized with secondary dopants or additives to achieve maximum ionic and electronic performance. The ability to attain higher resolution recordings through improved signal-to-noise ratio (SNR), along with the possibility of direct contact with the electrolyte or tissue and low needed driving voltages, add to the attractive nature of the OECT. Examples employing this technology to record electrophysiological signals with PEDOT-based OECTs include neural recordings from cortical devices (Section 3.2.3) [201,204,205], as well as cardiac signals [190]. To achieve the latter, OECT arrays for ECG signal recordings (Fig. 9e) were fabricated on bioresorbable transparent poly (L-lactide-co-glycolide) (PLGA) [190]. The importance of incorporating an epoxy crosslinker additive in the PEDOT:PSS suspension and maintaining pH neutral conditions were noted to be important in order to ensure the mechanical stability and adhesion to the substrate.

4.2.1. Artificial muscles/soft actuators

Human muscle accommodates large strain as a result of a chemical stimulus. To mimic the natural movement of a muscle, one approach is the use of soft electrodes that elongate or move when driven by an electric field without increasing in stiffness. Conducting polymers are promising candidates for this type of artificial muscle design, as well as for further electromechanical transduction applications (such as power generators), as they can reversibly change their dimensions upon electrochemical (de)doping at low voltages [206-209]. During electrochemical oxidation/reduction, ions and the associated solvent molecules from the surrounding electrolyte solution penetrate inside the polymer matrix. This ion flux has been suggested as the main cause for mechanical movement, as the reaction results in physical separation of the chains and large displacements in the volume of the film [210–212]. Layered structures may be constructed to take advantage of these physical changes within the film, producing microactuators intended (in some cases) for artificial muscle design. These are often tri-layered actuators in which at least two electrodes (cathode and anode) are necessary [213]. As an additional ion transport layer is also essential, CPs provide interesting candidate materials for the electrodes. Recent developments regarding ILs (discussed in Section 3.1.1) provide an excellent solution for the ion conduction layer and have driven artificial muscle design to a new level enabling performance in air. The solidstate electrolyte layer (i.e. IL) or a gel membrane is sandwiched between two CP films, and the motion of ions between the two films causes a deflection movement. In order to withstand the mechanical force resulting from this movement, the electrodes must be elastic and highly adhesive to the electrolyte layer in the middle. In 2012, Li et al. developed stretchable and highly conductive PEDOT/PSS films by adding sugar alcohols and monitoring the effects of temperature on the mechanical properties during subsequent heating of films [214,215]. In 2014 the same group made use of the modified PEDOT layers, separated by an ionic liquid/PU composite gel (i.e. the source of mobile ions), and applied a DC voltage to the electrodes (Fig. 10a) [216]. The resulting actuator bends towards the anode reversibly at low operation voltages (< 1.5 V) and functions up to 50 Hz. The mechanism of bending is mainly associated with the electric double layer and polarization caused by electrophoretic diffusion of ionic liquid in the PU matrix.

4.2.2. Tissue engineered conducting scaffolds

Research in the field of tissue engineering targets the production of artificial tissue that mimics the functionality and complexity of natural tissue. Engineered tissues can be used for pharmaceutical drug testing or can be implanted in the body where needed. In order to provide an environment outside of the body in which cells will grow in a more natural way, a scaffold is needed. This is a mechanical support which is similar to the extracellular matrix (ECM) surrounding cells in vivo, particularly at the initial stages of growth. Although flat surfaces, such as petri dishes, can supply mechanical support, it known that cells cultured on flat surfaces do not faithfully capture the physiological behavior of cells grown in vivo [217]. Moving from two-dimensional to three-dimensional (3D) substrates is one method to provide a more natural growth environment, thus eliciting a more physiological state of the resulting culture. Based on this, a large variety of 3D models have been developed, including scaffolds based on synthetic and bio-derived polymers. The mechanical properties of the scaffold material play a major role in determining cell adhesion, proliferation and functionality [218,219]. Indeed, it has been demonstrated that certain cell types only become functional on materials with a particular stiffness [220].

A variety of conducting scaffolds based on PEDOT have been

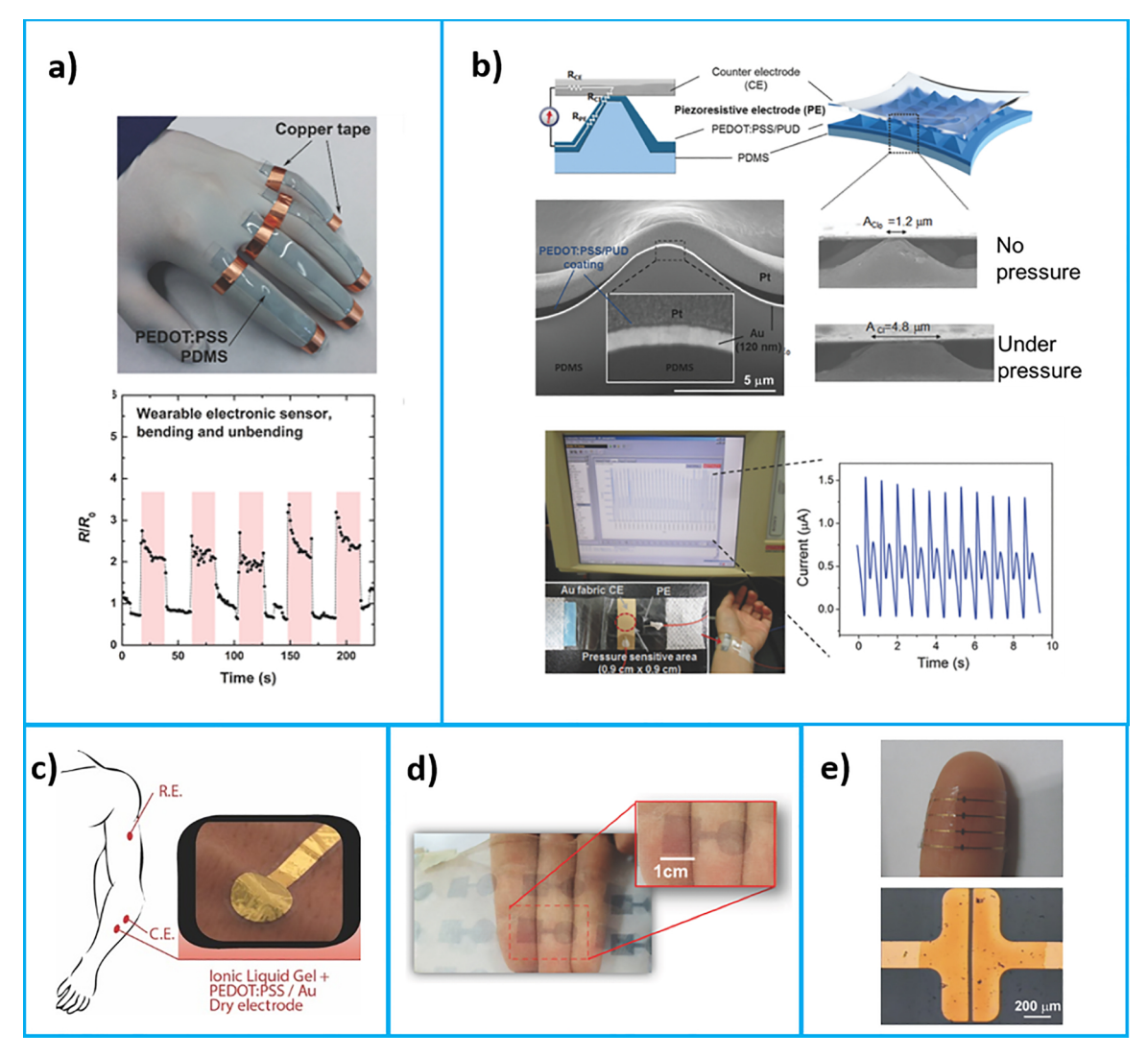


Fig. 9. a) Highly plasticized films of PEDOT:PSS act as a piezoresistive material. The skin-like resistive strain sensor can detect human motion. **Top**: Image of the device attached to a 1 mm thick PDMS substrate conforming to a human hand. **Bottom**: Plot of relative resistance (R/R₀) over time when repetitive strain is applied by bending of the fingers [21]. **b)** Overview of a stretchable resistive pressure sensor based on a PEDOT:PSS/PU thin film coating on PDMS pyramidal microstructures. **Top**: Sensor cross-section, which relies on changes in pyramid geometry in response to pressure. **Middle**: Scanning electron microscope (SEM) images show the dimensional change of the pyramid-shaped piezoresistive electrode with pressure. **Bottom**: The pressure sensor captures real-time arterial pulse waves from the wrist of the subject [129]. **c)** An EEG sensor based on PEDOT:PSS fabricated on a 2 μm thick parylene film [188]. **d)** PEDOT:PSS-based electrodes printed on a commercial textile with a zoomed view of an individual electrode. When wrapped around the finger the sensor measured ECG signals with high quality over 40 days [189]. **e)** An OECT with PEDOT:PSS as the active layer on a bioresorbable PLGA substrate, used for recording ECG signals [190]. Applications shown in **c)-e)** use PEDOT:PSS formulations incorporating silanes and the surfactant DBSA to enhance the mechanical properties of the film. Blue borders group images from specific studies.

Reproduced with permission of: [21,129,188–190] (For interpretation of the references to colour in this figure legend, the reader is referred to the web version of this article.).

prepared for interfacing cells *in vitro*, making use of straightforward modulation of mechanical properties [221,222]. A recent approach involves processing CPs in the form of foams/sponges [223]. Freeze casting a dispersion of PEDOT:PSS with a relatively high amount of the often employed silane-based crosslinker, GOPs, enables soft, porous, conducting foams, resilient to pressure and water (Fig. 10b) [224]. The pore size, density, softness and mechanical integrity of scaffolds are modified by the content of the crosslinker and the processing parameters. These scaffolds have been successfully used to host mammalian cells, which were also shown to be responsive to the oxidation state of the conducting network. The conducting scaffold was used in an impedance monitoring platform, signaling the presence of kidney endothelial cells [225]. The elasticity of the scaffold can be tailored to meet the needs of a particular cell type by the inclusion of collagen in the PEDOT:PSS dispersion. This not only reduces the Young's modulus

of the scaffolds, but may also improve the biocompatibility.

An alternate method for the development of 3D scaffolds involves the combination of PEDOT with hydrogel networks. A study by Teshimi, et al. incorporated PEDOT:PSS into a cross-linked silk fibroin hydrogel matrix, investigating the effects on electrical and mechanical properties, including variation of the mechanical stiffness as a result of silk fibroin content in the matrix. Using this method, microelectrodes for stimulation of primary neuronal cells were reported. The system additionally benefits from transparency of the materials, which allows for simultaneous electrical stimulation and fluorescence imaging (confocal laser scanning microscopy) of the voltage gated calcium channels expressed by the utilized Chinese hamster ovary (CHO) cells [226]. In a separate study, Green, et al. hybridized PEDOT with anionic hydrogels (heparin and PVA/heparin composites), which impart mechanical softness to the CP [178]. The resulting mechanical properties reach a

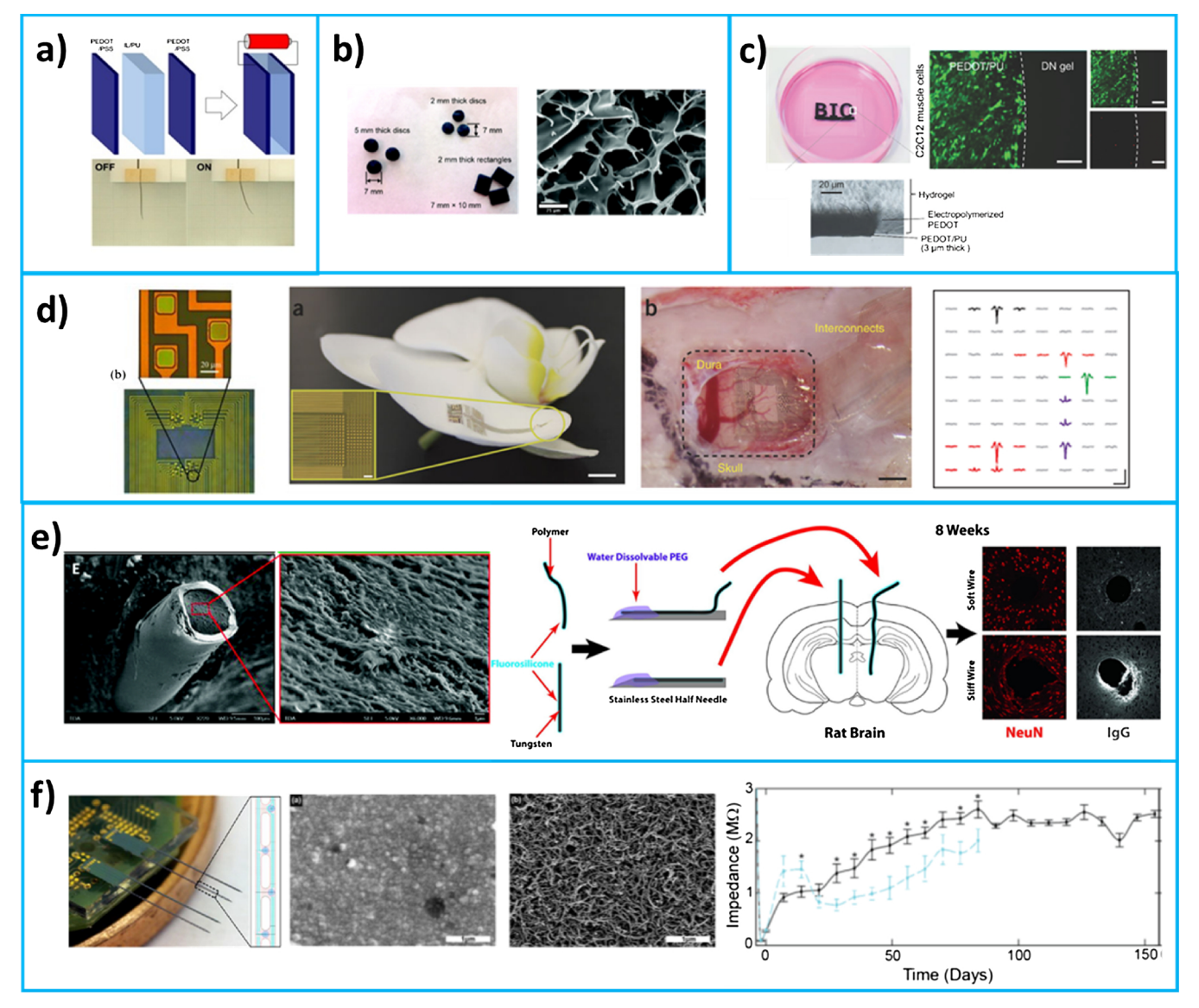


Fig. 10. a) Schematic illustration of a soft actuator fabricated by sandwiching an IL/PU gel between two sugar alcohol-plasticized PEDOT:PSS films. The photograph of the actuator shows the bending of the device with applied electric field, and its recovery after removal of the electric field [216]. b) GOPs modified PEDOT:PSS scaffold for engineering artificial tissues. The scaffold can be fabricated in different geometries. Young's modulus of the swollen scaffolds can be modulated through inclusion of a softer biomaterial in the composite, such as collagen [224]. c) A crossectional image of PEDOT:PSS/PU fabricated on a hydrogel. Fluorescent microscope images show attachment and proliferation of C2C12 muscle cells on the conducting hydrogel hybrid. Dual staining of cells was used to identify live (green) and dead (red) cells [227]. Scale bars are 200 μ m. d) PEDOT:PSS microelectrode array, fabricated on a parylene substrate. Left: The device conforms to the surface of an orchid petal (scale bar 5 mm). The inset is an optical micrograph of a 256-electrode ($10 \times 10 \mu$ m²) array (scale bar 100 μ m) [228]. Right: The device conforms to the surface of the rat somatosensory cortex and records single unit activity [199]. e) SEM images of the fluorosilicone-coated soft wire including a blend of PDMS and PEDOT-PEG polymer in its core. The soft microwire and a stiff tungsten wire were implanted into the rat brain using a shank. The number of neurons around soft implants was significantly higher than those around the stiff implants (NeuN staining) and soft microwire leads to less tissue damage after 8 weeks of implantation (IgG staining) [229]. f) PEDOT without (middle, left) and with CNTs (middle, right) showing good performance over multiple weeks implanted *in vivo* (right) [104]. Blue borders group images from specific studies.

Reproduced with permission of: [216,224,227,228,199,229,104] (For interpretation of the references to colour in this figure legend, the reader is referred to the web version of this article.).

modulus close to 2 MPa, softer than PEDOT:pTS film analogues, while maintaining similar electroactivity. Although PC12 cells showed similar adhesion behavior to these hydrogels when compared to pristine PEDOT:pTS surfaces, neurite growth was halved. Sasaki, et al. developed 3D conductive conduits composed of PEDOT/PU within a hydrogel matrix, which may be used as electrodes (Fig. 10c). These hybrids are autoclavable and biocompatible with muscle and neuronal cells. They display stable and highly conducting behavior over a range of physiological strain levels, however cell-loaded soft scaffolds have not yet been applied for electrical and mechanical stimulation

experiments [227]. The achievements to date in this area are promising, with room for improvement through further optimization of material properties and supplementary studies with various cell types.

4.2.3. Implantable electronics

Flexible and stretchable electronic devices offer great advantages when applied as neural interfaces. Intimate contact with the tissue improves the ability to record and stimulate activity of individual or selected populations of neurons. These devices may be used to map brain activity, restore motor function through spinal cord stimulation,

stimulate the heart to maintain a normal rhythm, or restore vision or hearing [230-233]. The stability, biocompatibility and long term functionality of the devices, which require a surgical operation for implantation, are much more critical when compared to skin-mounted devices. Excellent reviews on recent developments of implantable device technologies focus on the challenges that hinder widespread application in clinical environments [12,200,234]. One of the biggest issues for implantable electronics is the foreign body response of biological tissue to implants. The mechanical mismatch between the soft neural tissue and the rigid electronics generates glial scarring at the neural interface [200]. The resulting scar tissue creates a physical distance between the electrode array and neurons, reducing recording or stimulation efficiency. Due to the signal attenuation across this distance, the level of recorded brain signal drops and for stimulation applications a higher level of current/voltage must be applied to the tissue. As typically used metals are more than 4 orders of magnitude stiffer than neural tissue [235], soft materials are desired both for shuttles and recording electronics to reduce micromotion-induced tissue damage [229]. Due to their inherently softer nature, the potential of conducting polymers have been widely explored in the past two decades, aspiring to prevent glial scarring for long-term use [200]. PEDOT-based films have received a great deal of attention for this goal, although not only due to the possibility to attain softer mechanical properties. When coated on conventional metal or metal oxide probes, PEDOT has been shown to improve electrode characteristics by way of reduced electrochemical impedance at the neural tissue/electrode interface.

Surface electrode arrays represent the less invasive form of implantable neural electronics as they do not penetrate into the tissue. As electrocorticography (ECoG) arrays are placed directly on the cortex, they greatly benefit from the overall softness and flexibility of the materials, which enhances conformability to the brain surface [11]. The continuous close contact with cortical tissue, along with the possibility to reduce the electrochemical impedance of the electrode using CPs, are significant advantages for this technology. Over the last decade, a handful of research groups have developed PEDOT-based microelectrode ECoG arrays [228,236,237]. Castagnola et al. have developed electropolymerized PEDOT:CNT coatings on ECoG arrays employing polyimide substrates [236,238]. in vivo recordings of somatosensory evoked potentials elicited though multiwhisker deflections were shown with signal power in the 0-250 Hz band, enhanced by 3.4 fold, as well as a threefold increase in SNR when comparing PEDOT:CNT coatings to uncoated gold electrodes [238]. Khodagholy et al. developed an extremely flexible parylene-based system (2-4 µm overall thickness) as well as a sacrificial layer peel-off method to allow spin-coating of PEDOT electrode coatings (Fig. 10d). PEDOT:PSS films are cast from dispersions containing additives EG, DBSA, and GOPs and the resulting low-impedance ECoG microelectrodes, termed NeuroGrid, demonstrated the impressive ability to record single-unit activity from the surface of the rodent brain [199]. Additional work utilizing the same material system includes a demonstration of comparable signal quality from the surface grid when compared to a standard Ir penetrating depth probe as well as extension of the Neurogrid to studies of the human brain [228,239]. These are important results, demonstrating the advancements in research on neural interfaces and the progression towards clinical application of optimized systems. Finally, highly conformable arrays of OECTs using an analogous material system, including the same PEDOT composition in the channel, showed improved SNR of electrophysiological recordings when compared to PEDOT electrodes. This is due to the local amplification of the OECT and demonstrates the potential use of OECTs for in vivo recordings, which could potentially be used to record small and more local activity

Improvements in neural signal quality through the use of conducting polymer coatings on implantable depth probes have also been well demonstrated. Important points of progress include reduction of

Young's modulus to avoid the above mentioned foreign body response, reduction of electrochemical impedance to attain higher SNR of recorded signals, and long-term stability of the PEDOT films. A great deal of work has gone into investigations of various counterions, revealing that electropolymerized PEDOT performance depends largely on the dopant anion. PEDOT films become softer as the size of the counterion is reduced in the dry state, however performance in the hydrated state is much more applicable to bio-interfacing conditions [240]. Once the material is hydrated, the softness of the film depends more on the hydrophilicity of the dopant molecule regardless of its size. The use of PSS, for instance, was found to produce films with the lowest elastic modulus in the swollen state when compared to small ions [241].

The incorporation of additives or other materials, as discussed in Section 3, has been explored in order to attain higher levels of stability as well as improving mechanical elasticity of implantable probes [178,242]. An example application achieving softer implants, investigated by Kolercik et al., involves the fabrication of elastomeric PEDOT microwires. The wires possess an inner conductive core, comprised of PDMS and a lauryl terminated PEDOT-PEG copolymer, and an outer insulating fluorosilicone layer (Fig. 10e) [229]. The resulting microwires had a Young's modulus of ~970 kPa, five orders of magnitude lower than tungsten counterparts and the lowest among PEDOTbased neural electrodes thus far. By altering the ratio of elastomer to conducting polymer, the wires were optimized to exhibit low impendence while maintaining the flexibility of the elastomer. The conductivity remained constant through hundreds of bending/unbending cycles. Neural recordings from the rodent visual cortex were made, capturing activity resulting from drifting bar stimulation.

Although significant advancements have been made regarding the mechanical and electrical properties of PEDOT-based systems, a considerable obstacle lies in the long-term stability to promote application of the developed systems, a vital concern for chronic implantations. A great deal of improvement has been achieved through the use of additives or exchange of utilized dopant ions to increase the mechanical integrity and improve adhesion to substrates, however the majority of studies only show results for up to 1-2 weeks [22,46,47,51]. In 2016, Kozai et al. reported an impressive improvement in recording duration of up to 154 days through the use of PEDOT electropolymerized using CNTs functionalized with carboxylic acid groups (Fig. 10f) [104]. The use of CNTs mechanically reinforces the polymer and prevents cracking previously observed during chronic experiments. It should be noted that PEDOT:PSS without CNTs maintained lower impedance over the initial 84 days, however the signal quality of PEDOT/CNT electrodes was better along with the longer recording capability. Research to further improve device stability over time will be valuable in order to move from promising experimental results towards clinically usable bioelectronic devices [104,243,244].

4.3. Summary

In summary, modified PEDOT films hold the potential to positively impact a variety of research and production fields ranging from solar energy harvesting and display technologies to bioelectronics and soft robotics. In this section we have aimed to give an accurate overview of the influential bioelectronic applications that have benefitted from tailored PEDOT films. Through process modifications and/or application of additives, significant advancements have been made in this field through improvement of properties such as conductivity, Young's modulus, transparency, and mechanical/electrochemical stability. Further development of PEDOT, as well as new material systems, in the following years will be extremely interesting regarding advancements in bioelectronics.

Funding

This project has received funding from the European Union's

Horizon 2020 research and innovation programme under the Marie Sklodowska-Curie RISE grant IONBIKE agreement No 823989. DCM acknowledges support from the US National Science Foundation Division of Materials Research, Grants DMR-1505144 and DMR-1808048. SI acknowledges support from King Abdullah University of Science and Technology. JQ acknowledges support from the Advanced Materials Characterization Lab at the University of Delaware.

Declaration of Competing Interest

The authors declare that they have no known competing financial interests or personal relationships that could have appeared to influence the work reported in this paper.

Acknowledgement

The authors would like to thank Brett Moore, Adam Williamson, and Xenofon Strakosas for edits.

References

- [1] S. Choi, H. Lee, R. Ghaffari, T. Hyeon, D.-H. Kim, Adv. Mater. 28 (June(22)) (2016) 4203-4218.
- [2] N. Lu, D.-H. Kim, Soft Robot. 1 (1) (2014) 53-62.
- D.-H. Kim, J.-H. Ahn, W.M. Choi, H.-S. Kim, T.-H. Kim, J. Song, Y.Y. Huang, Z. Liu, C. Lu, J.A. Rogers, Science 320 (5875) (2008) 507-511.
- [4] T. Sekitani, T. Someya, Adv. Mater. 22 (20) (2010) 2228-2246.
- [5] J.Y. Oh, S. Kim, H.-K. Baik, U. Jeong, Adv. Mater. 28 (22) (2016) 4455-4461.
- [6] J.Y. Oh, M. Shin, J.B. Lee, J.-H. Ahn, H.K. Baik, U. Jeong, ACS Appl. Mater Interfaces 6 (9) (2014) 6954–6961.
- S. Savagatrup, A.S. Makaram, D.J. Burke, D.J. Lipomi, Adv. Funct. Mater. 24 (8) (2014) 1169-1181.
- Z. Yu, X. Niu, Z. Liu, Q. Pei, Adv. Mater. 23 (34) (2011) 3989-3994.
- [9] M.D. Dickey, Adv. Mater. (2017).
- [10] H. Stoyanov, M. Kollosche, S. Risse, R. Waché, G. Kofod, Adv. Mater. 25 (4) (2013) 578-583.
- [11] J. Rivnay, H. Wang, L. Fenno, K. Deisseroth, G.G. Malliaras, Sci. Adv. 3 (6) (2017) p. e1601649.
- [12] S.M. Wellman, J.R. Eles, K.A. Ludwig, J.P. Seymour, N.J. Michelson, W.E. McFadden, A.L. Vazquez, T.D. Kozai, Adv. Funct. Mater. (2017).
- [13] M.L. Hammock, A. Chortos, B.C.-K. Tee, J.B.-H. Tok, Z. Bao, Adv. Mater. 25 (42) (2013) 5997-6038.
- [14] T. Someya, Z. Bao, G.G. Malliaras, Nature 540 (7633) (2016) 379-385.
- [15] S.E. Root, S. Savagatrup, A.D. Printz, D. Rodriquez, D.J. Lipomi, Chem. Rev. 117 (9) (2017) 6467-6499.
- [16] M. Berggren, A. Richter-Dahlfors, Adv. Mater. 19 (October(20)) (2007)
- V. Karagkiozaki, P.G. Karagiannidis, M. Gioti, P. Kavatzikidou, D. Georgiou, E. Georgaraki, S. Logothetidis, Biochimica et Biophysica Acta (BBA) - General Subjects 1830 (September(9)) (2013) 4294-4304.
- [18] U. Lang, N. Naujoks, J. Dual, Synth. Met. 159 (March(5-6)) (2009) 473-479.
- [19] D. Tahk, H.H. Lee, D.-Y. Khang, Macromolecules 42 (18) (2009) 7079-7083.
- [20] J. Rivnay, R.M. Owens, G.G. Malliaras, Chem. Mater. 26 (2014) 679-685.
- [21] S. Savagatrup, E. Chan, S.M. Renteria-Garcia, A.D. Printz, A.V. Zaretski, T.F. O'Connor, D. Rodriquez, E. Valle, D.J. Lipomi, Adv. Funct. Mater. 25 (3) (2015) 427-436.
- [22] K.A. Ludwig, J.D. Uram, J. Yang, D.C. Martin, D.R. Kipke, J. Neural Eng. 3 (1) (2006) 59.
- [23] R. Kiebooms, A. Aleshin, K. Hutchison, F. Wudl, A. Heeger, Synth, Met. 101 (1-3) (1999) 436-437.
- [24] M. Culebras, C.M. Gomez, A. Cantarero, J. Mater. Chem. A 2 (26) (2014) 10109-10115.
- Y. Vlamidis, M. Lanzi, E. Salatelli, I. Gualandi, B. Fraboni, L. Setti, D. Tonelli, J. Solid State Electrochem, 19 (6) (2015) 1685-1693.
- [26] Z.U. Khan, O. Bubnova, M.J. Jafari, R. Brooke, X. Liu, R. Gabrielsson, T. Ederth, D.R. Evans, J.W. Andreasen, M. Fahlman, X. Crispin, J. Mater. Chem. C 3 (October (40)) (2015) 10616-10623.
- [27] S.A. Spanninga, D.C. Martin, Z. Chen, J. Phys. Chem. C 114 (35) (2010) 14992-14997
- [28] K.Z. Xing, M. Fahlman, X.W. Chen, O. Inganäs, W.R. Salaneck, Synth. Met. 89 (September(3)) (1997) 161-165.
- [29] I. Petsagkourakis, E. Pavlopoulou, G. Portale, B.A. Kuropatwa, S. Dilhaire,
- G. Fleury, G. Hadziioannou, Sci. Rep. 6 (July) (2016) p. srep30501. Y.-H. Ha, N. Nikolov, S.K. Pollack, J. Mastrangelo, B.D. Martin, R. Shashidhar, Adv. Funct. Mater. 14 (6) (2004) 615-622.
- [31] H. Yamato, K. Kai, M. Ohwa, T. Asakura, T. Koshiba, W. Wernet, Synth. Met. 83 (2) (1996) 125-130.
- [32] K. Sun, S. Zhang, P. Li, Y. Xia, X. Zhang, D. Du, F.H. Isikgor, J. Ouyang, J. Mater. Sci. Mater. Electron. 26 (July(7)) (2015) 4438-4462.

- [33] M. Asplund, E. Thaning, J. Lundberg, A.C. Sandberg-Nordqvist, B. Kostyszyn, O. Inganäs, H. von Holst, Biomed. Mater. 4 (4) (2009) p. 045009.
- [34] J.L. Bredas, G.B. Street, Acc. Chem. Res. 18 (10) (1985) 309-315.
- [35] O. Wei, M. Mukaida, K. Kirihara, Y. Naitoh, T. Ishida, Materials 8 (February(2)) (2015) 732–750.
- P.-H. Aubert, L. Groenendaal, F. Louwet, L. Lutsen, D. Vanderzande, G. Zotti, Synth. Met. 126 (2-3) (2002) 193-198.
- G. Zotti, S. Zecchin, G. Schiavon, F. Louwet, L. Groenendaal, X. Crispin, W. Osikowicz, W. Salaneck, M. Fahlman, Macromolecules 36 (9) (2003) 3337-3344.
- [38] V. Castagnola, E. Descamps, A. Lecestre, L. Dahan, J. Remaud, L.G. Nowak, C. Bergaud, Biosens. Bioelectron. 67 (2015) 450-457.
- A.I. Melato, M.H. Mendonça, L.M. Abrantes, J. Solid State Electrochem. 13 (3) (2009) 417-426.
- L. Ouyang, C. Kuo, B. Farrell, S. Pathak, B. Wei, J. Qu, D.C. Martin, J. Mater. Chem. B 3 (25) (2015) 5010-5020.
- H. Yamato, M. Ohwa, W. Wernet, J. Electroanal. Chem. 397 (1-2) (1995)
- [42] H. Yamato, K. Kai, M. Ohwa, W. Wernet, M. Matsumura, Electrochim. Acta 42 (16) (1997) 2517–2523.
- S.J. Wilks, S.M. Richardson-Burns, J.L. Hendricks, D.C. Martin, K.J. Otto, Front Neuroengineering 2 (June) (2009).
- [44] J. Yang, K. Lipkin, D.C. Martin, J. Biomater. Sci. Polym. Ed. 18 (8) (2007) 1075-1089
- J. Yang, D.H. Kim, J.L. Hendricks, M. Leach, R. Northey, D.C. Martin, Acta Biomater. 1 (1) (2005) 125-136.
- E.M. Thaning, M.L.M. Asplund, T.A. Nyberg, O.W. Inganäs, H. von Holst, J. Biomed. Mater. Res. 93B (May (2)) (2010) 407-415.
- S. Venkatraman, J. Hendricks, Z.A. King, A.J. Sereno, S. Richardson-Burns, D. Martin, J.M. Carmena, IEEE Trans. Neural Syst. Rehabil. Eng. 19 (June(3)) (2011) 307-316.
- [48] X. Cui, J.F. Hetke, J.A. Wiler, D.J. Anderson, D.C. Martin, Sens. Actuators A Phys. 93 (August(1)) (2001) 8-18.
- X. Cui, D.C. Martin, Sens. Actuators B Chem. 89 (March(1-2)) (2003) 92-102.
- Y.H. Xiao, C.M. Li, M.-L. Toh, R. Xue, J. Appl. Electrochem. 38 (December(12)) [50] (2008) 1735-1741.
- M. Asplund, H. von Holst, O. Inganäs, Biointerphases 3 (September(3)) (2008) **[51]** 83-93
- [52] M. Asplund, T. Nyberg, O. Inganäs, Polym. Chem. 1 (9) (2010) 1374–1391.
 [53] R. Lv, Y. Sun, F. Yu, H. Zhang, J. Appl. Polym. Sci. 124 (April(1)) (2012) 855–863.
 [54] F. Jonas, L. Schrader, Synth. Met. 41 (3) (1991) 831–836.

- [55] M. Fabretto, K. Zuber, C. Hall, P. Murphy, Macromol. Rapid Commun. 29 (16) (2008) 1403-1409
- [56] M.N. Gueye, A. Carella, N. Massonnet, E. Yvenou, S. Brenet, J. Faure-Vincent, S. Pouget, F. Rieutord, H. Okuno, A. Benayad, R. Demadrille, J.-P. Simonato, Chem. Mater. 28 (May (10)) (2016) 3462-3468.
- B. Winther-Jensen, D.W. Breiby, K. West, Synth. Met. 152 (1-3) (2005) 1-4.
- [58] B. Winther-Jensen, K. West, Macromolecules 37 (12) (2004) 4538–4543.
- [59] L. Groenendaal, F. Jonas, D. Freitag, H. Pielartzik, J.R. Reynolds, Adv. Mater. 12 (April(7)) (2000) 481-494.
- T. Park, C. Park, B. Kim, H. Shin, E. Kim, Energy Environ. Sci. 6 (February(3)) (2013) 788-792.
- X. Gong, P.K. Iyer, D. Moses, G.C. Bazan, A.J. Heeger, S.S. Xiao, Adv. Funct. Mater. 13 (4) (2003) 325-330.
- Y. Li, Y. Cao, J. Gao, D. Wang, G. Yu, A.J. Heeger, Synth. Met. 99 (February(3)) (1999) 243-248.
- [63] J. Gao, G. Yu, and A. J. Heeger, Advanced Materials, vol. 10, 9, pp. 692-695.
- S. Kirchmeyer, K. Reuter, J. Mater. Chem. 15 (21) (2005) 2077-2088.
- [65] A. Elschner, S. Kirchmeyer, W. Lovenich, U. Merker, K. Reuter, PEDOT: Principles and Applications of an Intrinsically Conductive Polymer, CRC Press, 2010.
- C. Badre, L. Marquant, A.M. Alsayed, L.A. Hough, Adv. Funct. Mater. 22 (July(13)) (2012) 2723-2727.
- Y. Xia, J. Ouyang, Org. Electron. 11 (June(6)) (2010) 1129-1135.
- Y. Xia, H. Zhang, J. Ouyang, J. Mater. Chem. 20 (November(43)) (2010) 9740-9747.
- J. Ouyang, Displays 34 (December(5)) (2013) 423-436.
- N. Kim, S. Kee, S.H. Lee, B.H. Lee, Y.H. Kahng, Y.-R. Jo, B.-J. Kim, K. Lee, Adv. Mater. 26 (April(14)) (2014) 2268-2272.
- J. Huang, P.F. Miller, M.J.C. De, M. De, D.D.C. Bradley, Synth. Met. 139 (3) (2003) 569-572.
- [72] B. Fan, X. Mei, J. Ouyang, Macromolecules 41 (August(16)) (2008) 5971–5973.
- [73] H. Shi, C. Liu, Q. Jiang, J. Xu, Adv. Electron. Mater. 1 (4) (2015).
- [74] Y. Ner, M.A. Invernale, J.G. Grote, J.A. Stuart, G.A. Sotzing, Synth. Met. 160 (March(5)) (2010) 351-353.
- Z. Guo, H. Liu, C. Jiang, Y. Zhu, M. Wan, L. Dai, L. Jiang, Small 10 (10) (2014) 2087-2095.
- D.G. Harman, R. Gorkin, L. Stevens, B. Thompson, K. Wagner, B. Weng, J.H.Y. Chung, M. in het Panhuis, G.G. Wallace, Acta Biomater. 14 (March) (2015)
- [77] F.N. Ajjan, N. Casado, T. Rębiś, A. Elfwing, N. Solin, D. Mecerreyes, O. Inganäs, J. Mater. Chem. A 4 (5) (2016) 1838-1847.
- M. Daniele, del A. Isabel, S. Wandert, D.-G. Javier, C. Begona, S. Haritz, M. David, Macromol. Biosci. 16 (August(8)) (2016) 1227-1238.
- M. Horikawa, T. Fujiki, T. Shirosaki, N. Ryu, H. Sakurai, S. Nagaoka, H. Ihara, J. Mater. Chem. C 3 (August(34)) (2015) 8881-8887.
- L. Zhang, M. Fairbanks, T.L. Andrew, Adv. Funct. Mater. 27 (May (24)) (2017).

- [81] J.P. Lock, S.G. Im, K.K. Gleason, Macromolecules 39 (16) (2006) 5326-5329.
- [82] M.E. Alf, A. Asatekin, M.C. Barr, S.H. Baxamusa, H. Chelawat, G. Ozaydin-Ince, C.D. Petruczok, R. Sreenivasan, W.E. Tenhaeff, N.J. Trujillo, S. Vaddiraju, J. Xu, K.K. Gleason, Adv. Mater. 22 (May (18)) (2010) 1993–2027.
- [83] C.F. Cullis, S. Kurmanadhan, Combust. Flame 31 (1978) 1-5.
- [84] A. Mohammadi, M.-A. Hasan, B. Liedberg, I. Lundström, W.R. Salaneck, Synth. Met. 14 (3) (1986) 189–197.
- [85] J. Kim, E. Kim, Y. Won, H. Lee, K. Suh, Synth. Met. 139 (2) (2003) 485-489.
- [86] L. Zhang, T.L. Andrew, Adv. Mater. Interfaces 4 (23) (2017) p. 1700873.
- [87] B. Winther-Jensen, J. Chen, K. West, G. Wallace, Macromolecules 37 (16) (2004) 5930-5935
- [88] P. Subramanian, N. Clark, B. Winther-Jensen, D. MacFarlane, L. Spiccia, Aust. J. Chem. 62 (2)) (2009) 133–139.
- [89] D. Evans, M. Fabretto, M. Mueller, K. Zuber, R. Short, P. Murphy, J. Mater. Chem. 22 (30) (2012) 14889–14895.
- [90] H. Chelawat, S. Vaddiraju, K. Gleason, Chem. Mater. 22 (May (9)) (2010) 2864–2868.
- [91] J.-Y. Kim, M.-H. Kwon, Y.-K. Min, S. Kwon, D.-W. Ihm, Adv. Mater. 19 (21) (2007) 3501–3506.
- [92] S.G. Im, K.K. Gleason, Macromolecules 40 (18) (2007) 6552-6556.
- [93] B. Cho, K.S. Park, J. Baek, H.S. Oh, Y.-E. Koo Lee, M.M. Sung, Nano Lett. 14 (June (6)) (2014) 3321–3327.
- [94] A.T. Lawal, G.G. Wallace, Talanta 119 (February) (2014) 133-143.
- [95] R. Brooke, P. Cottis, P. Talemi, M. Fabretto, P. Murphy, D. Evans, Prog. Mater. Sci. 86 (May) (2017) 127–146.
- [96] X.T. Cui, D.D. Zhou, IEEE Trans. Neural Syst. Rehabil. Eng. 15 (December(4)) (2007) 502–508.
- [97] R. Green, R.T. Hassarati, L. Bouchinet, C.S. Lee, G.L.M. Cheong, J.F. Yu, C.W. Dodds, G.J. Suaning, L. Poole-Warren, N.H. Lovell, Biomaterials 33 (25) (2012) 5875–5886.
- [98] A.S. Pranti, A. Schander, A. Bödecker, W. Lang, Sens. Actuators B Chem. 275 (December) (2018) 382–393.
- [99] X. Wang, L. Tao, Y. Hao, Z. Liu, H. Chou, I. Kholmanov, S. Chen, C. Tan, N. Jayant,
- Q. Yu, Small 10 (4) (2014) 694–698. [100] M.R. Abidian, J.M. Corey, D.R. Kipke, D.C. Martin, Small 6 (3) (2010) 421–429.
- [101] Y. Lu, Y. Li, J. Pan, P. Wei, N. Liu, B. Wu, J. Cheng, C. Lu, L. Wang, Biomaterials 33 (January(2)) (2012) 378–394.
- [102] C. Boehler, F. Oberueber, S. Schlabach, T. Stieglitz, M. Asplund, ACS Appl. Mater. Interfaces 9 (1) (2016) 189–197.
- [103] X. Luo, C.L. Weaver, D.D. Zhou, R. Greenberg, X.T. Cui, Biomaterials 32 (August (24)) (2011) 5551–5557.
- [104] T.D.Y. Kozai, K. Catt, Z. Du, K. Na, O. Srivannavit, R.M. Haque, J. Seymour, K.D. Wise, E. Yoon, X.T. Cui, IEEE Trans. Biomed. Eng. 63 (January(1)) (2016) 111–119.
- [105] Z. Wang, J. Xu, Y. Yao, L. Zhang, Y. Wen, H. Song, D. Zhu, Sens. Actuators B Chem. 196 (June) (2014) 357–369.
- [106] Z. Mekhalif, P. Lang, F. Garnier, J. Electroanal. Chem. 399 (December(1)) (1995) 61–70
- [107] S. Carli, L. Casarin, G. Bergamini, S. Caramori, C.A. Bignozzi, J. Phys. Chem. C 118 (July(30)) (2014) 16782–16790.
- [108] B. Wei, J. Liu, L. Ouyang, C.-C. Kuo, D.C. Martin, ACS Appl. Mater. Interfaces 7 (July(28)) (2015) 15388–15394.
- [109] L. Ouyang, B. Wei, C. Kuo, S. Pathak, B. Farrell, D.C. Martin, Sci. Adv. 3 (March (3)) (2017) p. e1600448.
- [110] D. Chhin, D. Polcari, C.B.-L. Guen, G. Tomasello, F. Cicoira, S.B. Schougaard, J. Electrochem. Soc. 165 (January(12)) (2018) G3066–G3070.
- [111] S. Ghosh, O. Inganäs, Synth. Met. 101 (May (1-3)) (1999) 413-416.
- [112] A. Håkansson, S. Han, S. Wang, J. Lu, S. Braun, M. Fahlman, M. Berggren, X. Crispin, S. Fabiano, J. Polym. Sci. Part B: Polym. Phys. 55 (May (10)) (2017) 814–820.
- [113] M. ElMahmoudy, S. Inal, A. Charrier, I. Uguz, G.G. Malliaras, S. Sanaur, Macromol. Mater. Eng. 302 (5) (2017).
- [114] E. Stavrinidou, P. Leleux, H. Rajaona, D. Khodagholy, J. Rivnay, M. Lindau, S. Sanaur, G.G. Malliaras, Adv. Mater. 25 (32) (2013).
- [115] X. Strakosas, B. Wei, D.C. Martin, R.M. Owens, J. Mater. Chem. B 4 (29) (2016) 4952–4968.
- [116] V.F. Curto, M.P. Ferro, F. Mariani, E. Scavetta, R.M. Owens, Lab Chip 18 (March (6)) (2018) 933–943.
- [117] I. del Agua, S. Marina, C. Pitsalidis, D. Mantione, M. Ferro, D. Iandolo, A. Sanchez-Sanchez, G.G. Malliaras, R.M. Owens, D. Mecerreyes, ACS Omega 3 (July(7)) (2018) 7424–7431.
- [118] D. Mawad, A. Lauto, G.G. Wallace, Conductive Polymer Hydrogels, Polymeric Hydrogels As Smart Biomaterials, Springer, Cham, 2016, pp. 19–44.
- [119] D. Mawad, A. Artzy-Schnirman, J. Tonkin, J. Ramos, S. Inal, M.M. Mahat, N. Darwish, L. Zwi-Dantsis, G.G. Malliaras, J.J. Gooding, A. Lauto, M.M. Stevens, Chem. Mater. 28 (17) (2016) 6080–6088.
- [120] I. del Agua, D. Mantione, N. Casado, A. Sanchez-Sanchez, G.G. Malliaras, D. Mecerreyes, ACS Macro Lett. 6 (April(4)) (2017) 473–478.
- [121] K.H. Skorenko, A.C. Faucett, J. Liu, N.A. Ravvin, W.E. Bernier, J.M. Mativetsky, W.E. Jones, Synth. Met. 209 (November) (2015) 297–303.
- [122] M. Fabretto, K. Zuber, C. Hall, P. Murphy, H.J. Griesser, J. Mater. Chem. 19 (42) (2009) 7871–7878.
- [123] M. Fabretto, M. Müller, K. Zuber, P. Murphy, Macromol. Rapid Commun. 30 (21) (2009) 1846–1851.
- [124] M. Fabretto, C. Jariego-Moncunill, J.-P. Autere, A. Michelmore, R.D. Short, P. Murphy, Polymer 52 (8) (2011) 1725–1730.

- [125] D. Bhattacharyya, R.M. Howden, D.C. Borrelli, K.K. Gleason, J. Polym. Sci. Part B: Polym. Phys. 50 (August(19)) (2012) 1329–1351.
- [126] S.G. Im, P.J. Yoo, P.T. Hammond, K.K. Gleason, Adv. Mater. 19 (October(19)) (2007) 2863–2867.
- [127] T.S. Hansen, K. West, O. Hassager, N.B. Larsen, Adv. Funct. Mater. 17 (16) (2007) 3069–3073.
- [128] H. Kai, W. Suda, Y. Ogawa, K. Nagamine, M. Nishizawa, ACS Appl. Mater. Interfaces (2017).
- [129] C.-L. Choong, M.-B. Shim, B.-S. Lee, S. Jeon, D.-S. Ko, T.-H. Kang, J. Bae, S.H. Lee, K.-E. Byun, J. Im, Adv. Mater. 26 (21) (2014) 3451–3458.
- [130] A. Maziz, C. Plesse, C. Soyer, C. Chevrot, D. Teyssié, E. Cattan, F. Vidal, Funct. Mater. 24 (August(30)) (2014) 4851–4859.
- [131] L.H. Sperling, Encyclopedia of Polymer Science and Technology (March) (2004).
- [132] M.Y. Teo, N. Kim, S. Kee, B.S. Kim, G. Kim, S. Hong, S. Jung, K. Lee, ACS Appl. Mater. Interfaces 9 (1) (2016) 819–826.
- [133] Y. Wang, C. Zhu, R. Pfattner, H. Yan, L. Jin, S. Chen, F. Molina-Lopez, F. Lissel, J. Liu, N.I. Rabiah, et al., Sci. Adv. 3 (3) (2017) p. e1602076.
- [134] D.J. Lipomi, B.C.-K. Tee, M. Vosgueritchian, Z. Bao, Adv. Mater. 23 (April(15)) (2011) 1771–1775.
- [135] T. Wang, Y. Qi, J. Xu, X. Hu, P. Chen, Appl. Surf. Sci. 250 (1) (2005) 188-194.
- [136] T. Tevi, S.W. Saint Birch, S.W. Thomas, A. Takshi, Synth. Met. 191 (May) (2014) 59–65.
- [137] X. Yan, L. Zhang, J. Appl. Electrochem. 43 (6) (2013) 605-610.
- [138] W. Lu, A.G. Fadeev, B. Qi, E. Smela, B.R. Mattes, J. Ding, G.M. Spinks, J. Mazurkiewicz, D. Zhou, G.G. Wallace, D.R. MacFarlane, S.A. Forsyth, M. Forsyth, Science 297 (5583) (2002) 983–987.
- [139] J.-S. Noh, Polymers 8 (April(4)) (2016) 123.
- [140] C.A. Lamont, O. Winther-Jensen, B. Winther-Jensen, J. Mater. Chem. B Mater. Biol. Med. 3 (October(43)) (2015) 8445–8448.
- [141] F. Boubée de Gramont, S. Zhang, G. Tomasello, P. Kumar, A. Sarkissian, F. Cicoira, Highly stretchable electrospun conducting polymer nanofibers, Appl. Phys. Lett. 111 (August(9)) (2017) p. 093701.
- [142] J. Lang, Udo, Dual, Mechanical properties of BAYTRON P, 2004 4th IEEE International Conference on Polymers and Adhesives in Microelectronics and Photonics: (Portland OR, 12-15 September 2004) (2004).
- [143] D. Rodriquez, J.-H. Kim, S.E. Root, Z. Fei, P. Boufflet, M. Heeney, T.-S. Kim, D.J. Lipomi, ACS Appl. Mater. Interfaces 9 (March(10)) (2017) 8855–8862.
- [144] J. Yang, D.C.D. Martin, J. Mater. Res. 21 (5) (2006) 1124-1132.
- [145] J. Qu, L. Ouyang, C. Kuo, D.C. Martin, Acta Biomater. 31 (February) (2016) 114–121.
- [146] A.D. Printz, A.V. Zaretski, S. Savagatrup, A.S.-C. Chiang, D.J. Lipomi, ACS Appl. Mater. Interfaces 7 (41) (2015) 23257–23264.
- [147] S.R. Dupont, M. Oliver, F.C. Krebs, R.H. Dauskardt, Sol. Energy Mater. Sol. Cells 97 (2012) 171–175.
- [148] S.R. Dupont, E. Voroshazi, P. Heremans, R.H. Dauskardt, Org. Electron. 14 (May (5)) (2013) 1262–1270.
- [149] C. Bruner, R. Dauskardt, Macromolecules 47 (3) (2014) 1117–1121.
- [150] J. Qu, N. Garabedian, D.L. Burris, D.C. Martin, J. Mech. Beh. Biomed. Mater. (2019), https://doi.org/10.1016/j.jmbbm.2019.103376.
- [151] J.E. Bartelt, M.R. Deakin, C. Amatore, R.M. Wightman, Anal. Chem. 60 (October (19)) (1988) 2167–2169.
- [152] G. Schiavon, S. Sitran, G. Zotti, Synth. Met. 32 (October(2)) (1989) 209–217.
- [153] G. Zotti, S. Zecchin, G. Schiavon, L. "Bert" Groenendaal, Chem. Mater. 12 (October (10)) (2000) 2996–3005.
- [154] M. Granström, O. Inganäs, Polymer 36 (15) (1995) 2867–2872.
- [155] D.C. Martin, J. Wu, C.M. Shaw, Z. King, S.A. Spanninga, S. Richardson-Burns, J. Hendricks, J. Yang, Polym. Rev. 50 (3) (2010) 340–384.
- [156] A.G. MacDiarmid, A.J. Epstein, Synth. Met. 65 (August(2)) (1994) 103-116.
- [157] X. Crispin, F.L.E. Jakobsson, A. Crispin, P.C.M. Grim, P. Andersson, A. Volodin, C. Van Haesendonck, M. Van der Auweraer, W.R. Salaneck, M. Berggren, Chem. Mater. 18 (18) (2006) 4354–4360.
- [158] J.Y. Kim, J.H. Jung, D.E. Lee, J. Joo, Synth. Met. 126 (2) (2002) 311-316.
- [159] F. Louwet, L. Groenendaal, J. D'Haen, J. Manca, L. Leenders, J. Van Luppen, E. Verdonck, PEDOT/PSS: Synthesis, Characterization, Properties and Applications, (2003).
- [160] S.K.M. Jönsson, J. Birgerson, X. Crispin, G. Greczynski, W. Osikowicz, A.W. Denier van der Gon, W.R. Salaneck, M. Fahlman, Synth. Met. 139 (August(1)) (2003) 1–10.
- [161] J. Ouyang, C.-W. Chu, F.-C. Chen, Q. Xu, Y. Yang, Adv. Funct. Mater. 15 (February (2)) (2005) 203–208.
- [162] O.P. Dimitriev, D.A. Grinko, Y. Noskov, N.A. Ogurtsov, A.A. Pud, Synth. Met. 159 (November(21)) (2009) 2237–2239.
- [163] J. Nevrela, M. Micjan, M. Novota, S. Kovacova, M. Pavuk, P. Juhasz, J. Kovac, J. Jakabovic, M. Weis, J. Polym. Sci. Part B: Polym. Phys. 53 (16) (2015) 1139–1146.
- [164] P. Wilson, C. Lekakou, J.F. Watts, Org. Electron. 14 (December(12)) (2013) 3277–3285.
- [165] L.A.A. Pettersson, S. Ghosh, O. Inganäs, Org. Electron. 3 (3) (2002) 143–148.
- [166] M. Donoval, M. Micjan, M. Novota, J. Nevrela, S. Kovacova, M. Pavuk, P. Juhasz, M. Jagelka, J. Kovac, J. Jakabovic, M. Cigan, M. Weis, Appl. Surf. Sci. 395 (2017) 86–91.
- [167] D. Alemu, H.-Y. Wei, K.-C. Ho, C.-W. Chu, Energy Environ. Sci. 5 (11) (2012) 9662–9671.
- [168] Y. Xia, J. Ouyang, Org. Electron. 13 (October(10)) (2012) 1785–1792.
- [169] J.-S. Yeo, J.-M. Yun, D.-Y. Kim, S.-S. Kim, S.-I. Na, Sol. Energy Mater. Sol. Cells 114 (July) (2013) 104–109.

- [170] S.G. Im, K.K. Gleason, E.A. Olivetti, Doping level and work function control in oxidative chemical vapor deposited poly (3,4-ethylenedioxythiophene), Appl. Phys. Lett. 90 (April (15)) (2007) p. 152112.
- [171] M. Fabretto, M. Müller, K. Zuber, P. Murphy, Macromol. Rapid Commun. 30 (November(21)) (2009) 1846–1851.
- [172] R. Brooke, M. Fabretto, P. Hojati-Talemi, P. Murphy, D. Evans, Polymer 55 (August(16)) (2014) 3458–3460.
- [173] M. Mueller, M. Fabretto, D. Evans, P. Hojati-Talemi, C. Gruber, P. Murphy, Polymer 53 (11) (2012) 2146–2151.
- [174] K. Zuber, M. Fabretto, C. Hall, P. Murphy, Macromol. Rapid Commun. 29 (18) (2008) 1503–1508.
- [175] M. Fabretto, M. Müller, C. Hall, P. Murphy, R.D. Short, H.J. Griesser, Polymer 51 (8) (2010) 1737–1743.
- [176] M. Vosgueritchian, D.J. Lipomi, Z. Bao, Adv. Funct. Mater. 22 (2) (2012) 421–428.
- [177] M.V. Fabretto, D.R. Evans, M. Mueller, K. Zuber, P. Hojati-Talemi, R.D. Short, G.G. Wallace, P.J. Murphy, Chem. Mater. 24 (20) (2012) 3998–4003.
- [178] R. A. Green, R. T. Hassarati, J. A. Goding, S. Baek, N. H. Lovell, P. J. Martens, and L. A. Poole-Warren, Macromolecular Bioscience, vol. 12, 4, pp. 494–501.
- [179] Y.-Y. Lee, H.-Y. Kang, S.H. Gwon, G.M. Choi, S.-M. Lim, J.-Y. Sun, Y.-C. Joo, Adv. Mater. 28 (February(8)) (2016) 1636–1643.
- [180] M.Z. Seyedin, J.M. Razal, P.C. Innis, G.G. Wallace, Adv. Funct. Mater. 24 (20) (2014) 2957–2966.
- [181] S.C.B. Mannsfeld, B.C.-K. Tee, R.M. Stoltenberg, C.V.H.-H. Chen, S. Barman, B.V.O. Muir, A.N. Sokolov, C. Reese, Z. Bao, Nat. Mater. 9 (10) (2010) 859–864.
- [182] M. Ramuz, B. C.-K. Tee, J. B.-H. Tok, and Z. Bao, Advanced Materials, vol. 24, no. 24, pp. 3223–3227.
- [183] A.V. Shirinov, W.K. Schomburg, Sens. Actuators A Phys. 142 (March(1)) (2008) 48–55.
- [184] F.-R. Fan, L. Lin, G. Zhu, W. Wu, R. Zhang, Z.L. Wang, Nano Lett. 12 (June(6)) (2012) 3109–3114.
- [185] G.S. Kelly, Altern. Med. Rev. 12 (March(1)) (2007) 49-62.
- [186] Y. Chen, B. Lu, Y. Chen, X. Feng, Sci. Rep. 5 (June) (2015) 11505.
- [187] C. Yu, Z. Wang, H. Yu, H. Jiang, Appl. Phys. Lett. 95 (14) (2009) 141912.
- [188] P. Leleux, C. Johnson, X. Strakosas, J. Rivnay, T. Hervé, R.M. Owens, G.G. Malliaras, Adv. Healthc. Mater. 3 (September(9)) (2014) 1377–1380.
- [189] E. Bihar, T. Roberts, E. Ismailova, M. Saadaoui, M. Isik, A. Sanchez-Sanchez, D. Mecerreyes, T. Hervé, J. B. D. Graaf, and G. G. Malliaras, Advanced Materials Technologies, vol. 2, 4, p. 1600251.
- [190] A. Campana, T. Cramer, D. T. Simon, M. Berggren, and F. Biscarini, Advanced Materials, vol. 26, 23, pp. 3874–3878.
- [191] T. Q. Trung, S. Ramasundaram, B.-U. Hwang, and N.-E. Lee, Advanced Materials, vol. 28, 3, pp. 502–509.
- [192] M.D. Fox, M.E. Raichle, Nat. Rev. Neurosci. 8 (9) (2007) 700–711.
- [193] P. Leleux, J.M. Badier, J. Rivnay, C. Bénar, T. Hervé, P. Chauvel, G.G. Malliaras, Adv. Healthc. Mater. 3 (April(4)) (2014) 490–493.
- [194] E. Bihar, T. Roberts, M. Saadaoui, T. Hervé, J. B. D. Graaf, and G. G. Malliaras, Advanced Healthcare Materials, vol. 6, no. 6, p. 1601167.
- [195] D. Pani, A. Dessì, J.F. Saenz-Cogollo, G. Barabino, B. Fraboni, A. Bonfiglio, IEEE Trans. Biomed. Eng. 63 (March(3)) (2016) 540–549.
- [196] T.I. Oh, S. Yoon, T.E. Kim, H. Wi, K.J. Kim, E.J. Woo, R.J. Sadleir, IEEE Trans. Biomed. Circuits Syst. 7 (2) (2013) 204–211.
- [197] S.K. Sinha, Y. Noh, N. Reljin, G.M. Treich, S. Hajeb-Mohammadalipour, Y. Guo, K.H. Chon, G.A. Sotzing, ACS Appl. Mater. Interfaces 9 (43) (2017) 37524–37528.
- [198] Y. Guo, M.T. Otley, M. Li, X. Zhang, S.K. Sinha, G.M. Treich, G.A. Sotzing, ACS Appl. Mater. Interfaces (2016).
- [199] D. Khodagholy, J.N. Gelinas, T. Thesen, W. Doyle, O. Devinsky, G.G. Malliaras, G. Buzsáki, Nat. Neurosci. 18 (2) (2015) 310.
- [200] R. Green, M.R. Abidian, Adv. Mater. 27 (46) (2015) 7620-7637.
- [201] J. Rivnay, P. Leleux, M. Ferro, M. Sessolo, A. Williamson, D.A. Koutsouras, D. Khodagholy, M. Ramuz, X. Strakosas, R.M. Owens, C. Benar, J.-M. Badier, C. Bernard, G.G. Malliaras, Sci. Adv. 1 (May (4)) (2015) p. e1400251.
- [202] D. Khodagholy, J. Rivnay, M. Sessolo, M. Gurfinkel, P. Leleux, L.H. Jimison, E. Stavrinidou, T. Herve, S. Sanaur, R.M. Owens, G.G. Malliaras, Nat. Commun. 4 (July) (2013).
- [203] M.J. Donahue, A. Williamson, X. Strakosas, J.T. Friedlein, R.R. McLeod, H. Gleskova, G.G. Malliaras, Adv. Mater. 29 (2017).
- [204] P. Leleux, J. Rivnay, T. Lonjaret, J.-M. Badier, C. Bénar, T. Hervé, P. Chauvel, and G. G. Malliaras, Advanced Healthcare Materials, vol. 4, 1, pp. 142–147.
- [205] D. Khodagholy, T. Doublet, P. Quilichini, M. Gurfinkel, P. Leleux, A. Ghestem, E. Ismailova, T. Hervé, S. Sanaur, C. Bernard, G.G. Malliaras, Nat. Commun. 4 (March) (2013) 1575.
- $[206]\;$ E. Smela, Advanced Materials, vol. 15, 6, pp. 481–494.
- [207] H. Okuzaki, H. Suzuki, T. Ito, Synth. Met. 159 (November(21)) (2009) 2233–2236.
- [208] G. M. Spinks, G. G. Wallace, L. Liu, and D. Zhou, Macromolecular Symposia, vol. 192, 1, pp. 161–170.
- [209] F. Carpi, D.D. Rossi, R. Kornbluh, R.E. Pelrine, P. Sommer-Larsen, Dielectric Elastomers As Electromechanical Transducers: Fundamentals, Materials, Devices, Models and Applications of an Emerging Electroactive Polymer Technology, Elsevier, 2011.
- [210] E. Smela, O. Inganäs, I. Lundström, Science 268 (5218) (1995) 1735–1738.
- [211] T. Mirfakhrai, J.D.W. Madden, R.H. Baughman, Mater. Today 10 (April(4)) (2007) 30–38.
- [212] R.H. Baughman, Synth. Met. 78 (April(3)) (1996) 339-353.
- [213] R. Temmer, A. Maziz, C. Plesse, A. Aabloo, F. Vidal, T. Tamm, Smart Mater. Struct. 22 (10) (2013) 104006.
- [214] H. Okuzaki, Y. Harashina, H. Yan, Eur. Polym. J. 45 (January(1)) (2009) 256–261.

- [215] Y. Li, Y. Masuda, Y. Iriyama, H. Okuzaki, Trans. Mater. Res. Soc. Jpn. 37 (2) (2012) 303–306.
- [216] Y. Li, R. Tanigawa, H. Okuzaki, Smart Mater. Struct. 23 (7) (2014) p. 074010.
- [217] B.M. Baker, C.S. Chen, J. Cell. Sci. 125 (July(13)) (2012) 3015-3024.
- [218] D.E. Discher, P. Janmey, Y. Wang, Science 310 (5751) (2005) 1139-1143.
- [219] U. Fernekorn, J. Hampl, C. Augspurger, C. Hildmann, F. Weise, M. Klett, A. Läffert, M. Gebinoga, A. Williamson, A. Schober, RSC Adv. 3 (August(37)) (2013) 16558–16568.
- [220] A.J. Engler, S. Sen, H.L. Sweeney, D.E. Discher, Cell 126 (August(4)) (2006) 677–689.
- [221] A. Shahini, M. Yazdimamaghani, K.J. Walker, M.A. Eastman, H. Hatami-Marbini, B.J. Smith, J.L. Ricci, S.V. Madihally, D. Vashaee, L. Tayebi, Int. J. Nanomedicine 9 (December) (2013) 167–181.
- [222] A.G. Guex, J.L. Puetzer, A. Armgarth, E. Littmann, E. Stavrinidou, E.P. Giannelis, G.G. Malliaras, M.M. Stevens, Acta Biomater. 62 (October) (2017) 91–101.
- [223] X. Zhang, C. Li, Y. Luo, Langmuir 27 (5) (2011) 1915-1923.
- [224] A.M.-D. Wan, S. Inal, T. Williams, K. Wang, P. Leleux, L. Estevez, E.P. Giannelis, C. Fischbach, G.G. Malliaras, D. Gourdon, J. Mater. Chem. B Mater. Biol. Med. 3 (June(25)) (2015) 5040–5048.
- [225] S. Inal, A. Hama, M. Ferro, C. Pitsalidis, J. Oziat, D. Iandolo, A.-M. Pappa, M. Hadida, M. Huerta, D. Marchat, P. Mailley, and R. M. Owens, Advanced Biosystems, vol. 1, 6, p. 1700052.
- [226] T. Teshima, H. Nakashima, N. Kasai, S. Sasaki, A. Tanaka, S. Tsukada, and K. Sumitomo, Advanced Functional Materials, vol. 26, 45, pp. 8185–8193.
- [227] M. Sasaki, B.C. Karikkineth, K. Nagamine, H. Kaji, K. Torimitsu, M. Nishizawa, Adv. Healthc. Mater. 3 (11) (2014) 1919–1927.
- [228] D. Khodagholy, T. Doublet, M. Gurfinkel, P. Quilichini, E. Ismailova, P. Leleux, T. Herve, S. Sanaur, C. Bernard, G.G. Malliaras, Adv. Mater. 23 (36) (2011) 268–272.
- [229] C.L. Kolarcik, S. Lueben, S.A. Sapp, J. Hanner, N. Snyder, T.D.Y. Kozai, E. Chang, J.A. Nabity, S.T. Nabity, C.F. Lagenaur, X.T. Cui, S.D. Luebben, S.A. Sapp, J. Hanner, N. Snyder, T.D.Y. Kozai, E. Chang, J.A. Nabity, S.T. Nabity, C.F. Lagenaur, X.T. Cui, Soft Matter 11 (24) (2015) 4847–4861.
- [230] G.G. Wallace, S.E. Moulton, G.M. Clark, Science 324 (5924) (2009) 185-186.
- [231] J.-S. Noh, RSC Adv. 4 (4) (2014) 1857-1863.
- [232] S. M. Won, E. Song, J. Zhao, J. Li, J. Rivnay, and J. A. Rogers, Advanced Materials, vol. 0, no. 0, p. 1800534.
- [233] M. D. Ferro and N. A. Melosh, Advanced Functional Materials, vol. 28, 12, p. 1704335.
- [234] A. Gilletti, J. Muthuswamy, J. Neural Eng. 3 (3) (2006) 189.
- [235] R.T. Hassarati, W.F. Dueck, C. Tasche, P.M. Carter, L.A. Poole-Warren, R.A. Green, IEEE Trans. Neural Syst. Rehabil. Eng. 22 (March(2)) (2014) 411–418.
- [236] E. Castagnola, L. Maiolo, E. Maggiolini, A. Minotti, M. Marrani, F. Maita, A. Pecora, G.N. Angotzi, A. Ansaldo, L. Fadiga, G. Fortunato, D. Ricci, Ultraflexible and brain-conformable micro-electrocorticography device with low impedance PEDOT-carbon nanotube coated microelectrodes, 2013 6th International IEEE/EMBS Conference on Neural Engineering (NER) (2013) 927–930.
- [237] M.J. Donahue, A. Kaszas, G.F. Turi, B. Rózsa, A. Slézia, I. Vanzetta, G. Katona, C. Bernard, G.G. Malliaras, A. Williamson, eNeuro (December) (2018) p. ENEURO.0187-18.2018.
- [238] E. Castagnola, L. Maiolo, E. Maggiolini, A. Minotti, M. Marrani, F. Maita, A. Pecora, G.N. Angotzi, A. Ansaldo, M. Boffini, L. Fadiga, G. Fortunato, D. Ricci, Ieee Trans. Neural Syst. Rehabil. Eng. 23 (May (3)) (2015) 342–350.
- [239] D. Khodagholy, J.N. Gelinas, Z. Zhao, M. Yeh, M. Long, J.D. Greenlee, W. Doyle, O. Devinsky, G. Buzsaki, Sci. Adv. 2 (November) (2016) pp. e1601027–e1601027.
- [240] S. Baek, R.A. Green, L.A. Poole-Warren, J. Biomed. Mater. Res. 102 (August(8)) (2014) 2743–2754.
- [241] R.T. Hassarati, J.A. Goding, S. Baek, A.J. Patton, L.A. Poole-Warren, R.A. Green, J. Polym. Sci. Part B: Polym. Phys. 52 (9) (2014) 666–675.
- [242] K.D. Harris, A.L. Elias, H.-J. Chung, J. Mater. Sci. 51 (March(6)) (2016) 2771–2805.
- [243] N. Alba, Z. Du, K. Catt, T. Kozai, X. Cui, Biosensors 5 (4) (2015) 618-646.
- [244] R. Gerwig, K. Fuchsberger, B. Schroeppel, G.S. Link, G. Heusel, U. Kraushaar, W. Schuhmann, A. Stett, M. Stelzle, Front. Neuroeng. 5 (2012) 8.
- [245] Y.H. Kim, C. Sachse, M.L. Machala, C. May, L. Müller-Meskamp, K. Leo, Adv. Funct. Mater. 21 (6) (2011) 1076–1081.



Mary J. Donahue is an Assistant Professor in the Department of Bioelectronics (BEL) at the Centre Microèlectronique de Provence of the Ecole Nationale Supèrieure des Mines de Saint Étienne. She received a BS in Electrical Engineering and a BS in Computer Science, and MS in Electrical Engineering from Texas Tech University (Lubbock, TX USA). In 2006 she was awarded a Fulbright Scholarship to work at the Center for Micro- and Nanotechnology (ZMN) at the Technical University of Ilmenau, Germany, where she subsequently also completed her PhD. She joined BEL in 2014 and her current research interests include implantable organic sensors and the functionalization of organic transistors for *in vitro* and *in*

vivo Neuroengineering applications.



Ana Sanchez-Sanchez received her BS in Chemistry and her MS in Nanoscience from the University of the Basque Country (UPV-EHU). She earned her PhD in Physics of Nanostructures and Advanced Materials where she worked in the assembly and disassembly of bioinspired single chain polymer nanoparticles. As a postdoc, she worked on the synthesis and applications of innovative conductive biopolymeric materials. As a Marie Curie research Fellow at the University of Cambridge she worked on the fabrication of wearable electrodes for cutaneous electrophysiology. Her current research involves new conducting materials with applications for health monitoring and treatment.



Sahika Inal is an Assistant Professor of Bioengineering with affiliations in Electrical Engineering and Materials Science and Engineering at King Abdullah University of Science and Technology (KAUST). Prior to joining KAUST, she was a postdoctoral fellow in the Department of Bioelectronics at the Center of Microelectronics of Provence of the Ecole Nationale Supérieure des Mines de Saint-Étienne (Gardanne, France). She received her B.Sc. degree in Textile Engineering from Istanbul Technical University (2007, Istanbul, Turkey), her M.Sc. in Polymer Science and PhD in Experimental Physics from the University of Potsdam (2013, Potsdam, Germany). Her expertise is in polymer science and bioelectronic devices, particularly in photophysics of

conjugated polymers, characterization of polymer thin films and the design of biosensors and actuators. She currently investigates ion/electron conduction in organic electronic materials and designs bioelectronic devices that can record/stimulate biological signals. She leads the *Organic Bioelectronics* group at KAUST.



Jing Qu is a staff scientist of the Advanced Materials Characterization Lab (AMCL) at the University of Delaware. She received her Ph.D. in materials science and engineering at the University of Delaware in 2017 and joined the AMCL as a research scientist subsequently. Her research interests include the development of conducting polymers especially polythiophenes to improve their conductivity and durability in bioelectronic device applications. She has developed methods to quantitatively correlate the mechanical properties and durability of polythiophenes.



Róisín M. Owens is a University Lecturer at the Dept. of Chemical Engineering and Biotechnology in the University of Cambridge and a Fellow of Newnham College. She received her BA in Natural Sciences (Mod. Biochemistry) at Trinity College Dublin, and her PhD in Biochemistry and Molecular Biology at Southampton University. She carried out two postdoc fellowships at Cornell University and from 2009 to 2017 she was a group leader in the Department of Bioelectronics at Ecole des Mines de St. Etienne, on the microelectronics campus in Provence. Her current research centers on application of organic electronic materials for monitoring biological systems *in vitro*, with a specific interest in studying the gut-brain-microbiome axis. She has

received several awards including the European Research Council starting (2011), proof of concept grant (2014) and consolidator (2016) grants, a Marie Curie fellowship, and an

EMBO fellowship. In 2014, she became principle editor for biomaterials for MRS communications (Cambridge University Press), and she serves on the advisory board of Advanced BioSystems and Journal of Applied Polymer Science (Wiley). She is a 2019 laureate of the Suffrage Science award.



David Mecerreyes is an Ikerbasque Research Professor at POLYMAT- University of the Basaque Country (Spain). He received his PhD from University of Liege in 1998. After a postodoc (1998–2000) at IBM Almaden Research Center (California), he moved back to Spain to work at CIDETEC, Centre for Electrochemical Technologies. In 2010, he moved to POLYMAT, Basque Center for Macromolecular Design and Engineering where he became the leader of the Innovative Polymers Group. His expertise is in polymer synthesis of electroactive polymers such as poly(ionic liquid)s, polymer electrolytes, redox polymers and PEDOT type conductive polymers. Current research interests involve the application of innovative polymers in emerging

technologies such as organic batteries and bioelectronic devices.



George Malliaras is the Prince Philip Professor of Technology at the University of Cambridge (UK). He received a BS in Physics from the Aristotle University (Greece) in 1991, and a PhD in Mathematics and Physical Sciences, cum laude, from the University of Groningen (the Netherlands) in 1995. After postdocs at the University of Groningen and at the IBM Almaden Research Center (California), he joined the faculty in the Department of Materials Science and Engineering at Cornell University (New York) in 1999. From 2006 to 2009 he served as the Lester B. Knight Director of the Cornell NanoScale Science & Technology Facility. He moved to the Ecole des Mines de St. Etienne (France) in 2009 where he started the

Department of Bioelectronics and served as Department Head. He joined the University of Cambridge in 2017. His research on organic electronics and bioelectronics has been recognized with awards from the New York Academy of Sciences, the US National Science Foundation, and DuPont. He is a Fellow of the Materials Research Society and of the Royal Society of Chemistry and serves as an Associate Editor of Science Advances.



Prof. David C. Martin is the Associate Dean for Research and Entrepreneurship in the College of Engineering, Karl W. and Renate Böer Professor of Materials Science and Engineering, and Professor of Biomedical Engineering at the University of Delaware. He received his PhD in 1990 from the University of Massachusetts at Amherst. Afterward, he worked at the University of Michigan in Ann Arbor, MI, and was a Co-Founder and Chief Scientific Officer for Biotectix LLC, of Quincy, MA before it was fully acquired by Hereaus Medical Devices. His research interests include the development of conducting polymer coating for integrating biomedical devices in living tissue, high-resolution microscopy and impedance spectroscopy studies of

defects in ordered polymers and organic semiconductors, and the deformation behavior of crystalline polymer and organic molecular materials near surfaces. His research has been supported by the National Science Foundation, the Defense Advanced Research Projects Agency, the Army Research Office, and the National Institutes of Health. He is a Fellow of the American Chemical Society, the American Institute for Medical and Biological Engineering, and the American Physical Society.